

Original Paper

Early Holocene M~6 explosive eruption from Plosky volcanic massif (Kamchatka) and its tephra as a link between terrestrial and marine paleoenvironmental records

Vera Ponomareva¹, Maxim Portnyagin^{2,3}, Alexander Derkachev⁴, I. Florin Pendea⁵, Joanne Bourgeois⁶, Paula J. Reimer⁷, Dieter Garbe-Schönberg⁸, Stepan Krasheninnikov³ and Dirk Nürnberg²

- (1) Institute of Volcanology and Seismology, Petropavlovsk-Kamchatsky, Russia
- (2) Helmholtz-Zentrum für Ozeanforschung Kiel (GEOMAR), Kiel, Germany
- (3) V.I. Vernadsky Institute of Geochemistry and Analytical Chemistry, Moscow, Russia
- (4) V.I. Il'ichev Pacific Oceanological Institute, Vladivostok, Russia
- (5) Department of Interdisciplinary Studies, Lakehead University, Orillia, ON, Canada
- (6) Department of Earth and Space Sciences, University of Washington, Seattle, WA, USA
- (7) School of Geography, Archaeology and Palaeoecology, Queen's University Belfast, Belfast, Northern Ireland, UK
- (8) Institute of Geoscience, Christian-Albrechts-University of Kiel, 24118 Kiel, Germany

Vera Ponomareva

Email: vera.ponomareva1@gmail.com

Received: 29 November 2012

Accepted: 24 March 2013

Published online: 18 April 2013

Abstract

We report tephrochronological and geochemical data on early Holocene activity from Plosky volcanic massif in the Kliuchevskoi volcanic group, Kamchatka Peninsula. Explosive activity of this volcano lasted for ~1.5 kyr, produced a series of widely dispersed tephra layers, and was followed by profuse low-viscosity lava flows. This eruptive episode started a major reorganization of the volcanic structures in the western part of the Kliuchevskoi volcanic group. An explosive eruption from Plosky (M~6), previously unstudied, produced tephra (coded PL2) of a volume of 10–12 km³ (11–13 Gt), being one of the largest Holocene explosive eruptions in

Kamchatka. Characteristic diagnostic features of the PL2 tephra are predominantly vitric sponge-shaped fragments with rare phenocrysts and microlites of plagioclase, olivine and pyroxenes, medium- to high-K basaltic andesitic bulk composition, high-K, high-Al and high-P trachyandesitic glass composition with $\text{SiO}_2 = 57.5\text{--}59.5$ wt%, $\text{K}_2\text{O} = 2.3\text{--}2.7$ wt%, $\text{Al}_2\text{O}_3 = 15.8\text{--}16.5$ wt%, and $\text{P}_2\text{O}_5 = 0.5\text{--}0.7$ wt%. Other diagnostic features include a typical subduction-related pattern of incompatible elements, high concentrations of all REE ($>10\times$ mantle values), moderate enrichment in LREE (La/Yb ~ 5.3), and non-fractionated mantle-like pattern of LILE. Geochemical fingerprinting of the PL2 tephra with the help of EMP and LA-ICP-MS analyses allowed us to map its occurrence in terrestrial sections across Kamchatka and to identify this layer in Bering Sea sediment cores at a distance of >600 km from the source. New high-precision ^{14}C dates suggest that the PL2 eruption occurred $\sim 10,200$ cal BP, which makes it a valuable isochrone for early Holocene climate fluctuations and permits direct links between terrestrial and marine paleoenvironmental records. The terrestrial and marine ^{14}C dates related to the PL2 tephra have allowed us to estimate an early Holocene reservoir age for the western Bering Sea at $1,410 \pm 64$ ^{14}C years. Another important tephra from the early Holocene eruptive episode of Plosky volcano, coded PL1, was dated at 11,650 cal BP. This marker is the oldest geochemically characterized and dated tephra marker layer in Kamchatka to date and is an important local marker for the Younger Dryas—early Holocene transition. One more tephra from Plosky, coded PL3, can be used as a marker northeast of the source at a distance of ~ 110 km.

Electronic supplementary material

The online version of this article (doi:10.1007/s00531-013-0898-0) contains supplementary material, which is available to authorized users.

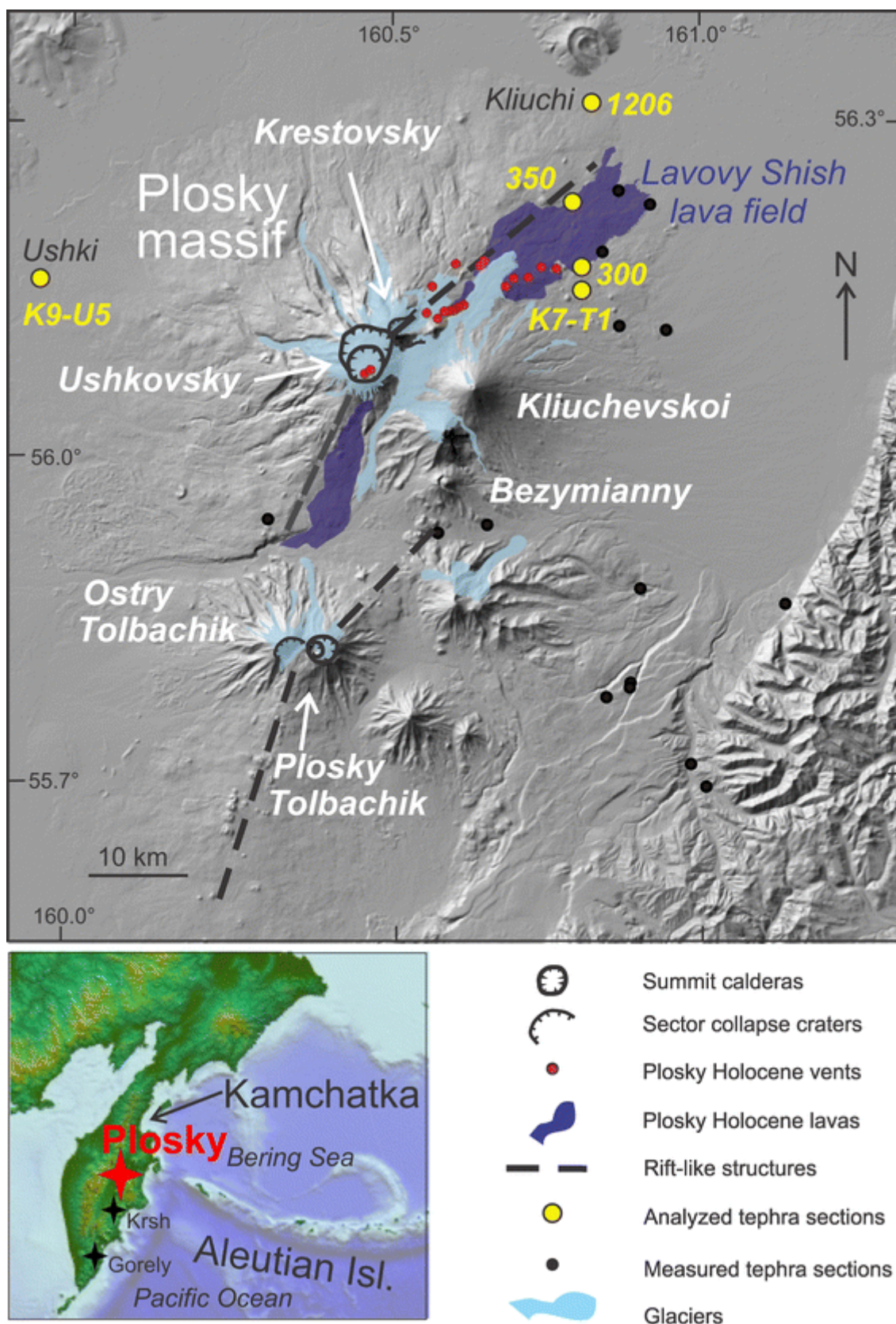
Keywords Tephra – Kamchatka – Marine cores – Bering Sea – Isochrones

Introduction

Many arc volcanoes are highly explosive and produce voluminous eruptions which may affect climate patterns due to wide dispersal of their tephra and associated aerosols. Existing records of past eruptions, however, are far from being complete, which hampers our understanding of climate-volcano interplay. More than that, volumes of many island arc tephra are likely underestimated because most of the tephra are carried offshore, so special terrestrial–marine tephra correlations are necessary to assess total eruptive volumes and calculate magma output from explosive eruptions. Also, tephra layers from large eruptions cover broad areas and may serve as isochrones providing direct links between terrestrial and submarine depositional successions. Research on the chronology and geochemical makeup of past eruptions as well as on their eruptive volumes and magnitudes contributes substantially to a better understanding of global paleovolcanic patterns and provides a tephrochronological framework for further

volcanological and paleoenvironmental studies.

The Kamchatka Peninsula (Fig. 1) hosts a highly active volcanic arc where most of the larger explosive eruptions produced pumice, characterized by andesitic-rhyolitic bulk compositions (Braitseva et al. 1997b) and by rhyolitic glass (Kyle et al. 2011). Decades of tephrochronological studies in Kamchatka have permitted documentation of 40 large Holocene explosive eruptions, with tephra volumes ranging from 170 to 0.5 km³ (Braitseva et al. 1997a, b, 1998; Ponomareva et al. 2007a). Tephra of these eruptions is widely used for dating and correlating various terrestrial deposits and landforms (e.g., Pinegina and Bourgeois 2001; Bourgeois et al. 2006; Braitseva et al. 1983, 1995, 1998; Kozhurin et al. 2006; Ponomareva 1990). Two particular periods of high-volume explosive eruptions with bulk tephra volumes of 10–170 km³ were identified and dated at ~8,700–6,800 and 1,750–1,250 cal BP (Braitseva et al. 1995; Ponomareva et al. 2007a).

**Fig. 1**

Top Digital elevation map showing Kliuchevskoi volcanic group with active volcanoes labeled. Note nested summit calderas on Ushkovskiy and Plosky Tolbachik and sector collapse craters on Krestovskiy and Ostry Tolbachik. Plosky massif comprises Ushkovskiy and Krestovskiy volcanoes; its Holocene vents are shown with *red circles* and their lava flows are shown in *purple*. Locations of tephra sections with measured early Holocene Plosky package are shown with *black filled circles*, and locations of the sections where Plosky tephra have been analyzed with *yellow filled circles*. Numbers of sections with analyzed Plosky tephra are given next to each *circle*. *Dashed black lines* show approximate directions of the arcuate rift-like structures that cross Ushkovskiy and Plosky Tolbachik volcanoes (according to

Melekestsev et al. 1974). Glaciers are shown in *light blue*. *Bottom* position of the Plosky volcanic massif relative to the Aleutian–Kamchatka arc junction. Other volcanoes mentioned in the text are Gorely and Krasheninnikov (Krsh at the figure)

Early Holocene (12–10 cal ka BP) explosive volcanism in Kamchatka is less well known because of poorer preservation of related deposits. The general belief is that this time was characterized by dominantly moderate, mafic, cone-building eruptions with very few, if any, large explosive events (e.g., Braitseva et al. 1995). A better understanding of volcanic activity and improved estimates of volcanic flux for early Holocene time may also offer a clue to the relationships between volcanism and glacial unloading (e.g., Jull and McKenzie 1996). Moreover, well-documented tephra markers for this period may serve as sensitive isochrones necessary in the study of rapid climate fluctuations recorded in various terrestrial and marine sediments.

In this paper, we document an early Holocene activity of Plosky volcanic massif (Kliuchevskoi volcanic group, Kamchatka) which produced a series of widely dispersed tephra layers and was followed by profuse lava flows. We provide mineralogical and geochemical data on proximal Plosky tephra (both bulk tephra and individual glass shards) that permit fingerprinting of individual tephra layers and correlation of three of them over the affected area. We reconstruct the parameters of a major Plosky eruption (coded PL2) and show that PL2 was one of the largest Holocene explosive events in the NW Pacific. Geochemically fingerprinted and dated Plosky tephra layers may serve as valuable isochrones for paleoclimate research. Correlation of PL2 tephra between terrestrial and marine sediments allows us to provide the first-ever estimate of ^{14}C reservoir age for the western Bering Sea.

Location and geological context

Plosky volcanic massif is a huge, complex edifice which occupies the northwestern sector of a highly productive volcanic cluster (Kliuchevskoi volcanic group), located close to the Kamchatka–Aleutian Arc junction (Figs. 1, 2). Plosky along with the Tolbachik volcanoes (Fig. 1) is positioned at the rear of the arc, ~180 km above the subduction zone (Gorbatov et al. 1997). Surprisingly little is known about Plosky activity considering its key geodynamic position, enormous volume, and some juvenile volcanic features on its slopes. The whole edifice is built on top of the mid-Pleistocene lava plateau underlying Kliuchevskoi volcanic group (Melekestsev et al. 1974). Based on its morphology and the stratigraphic relationship of its lavas with Last Glacial Maximum deposits, Plosky is believed to consist of a $90 \times 50 \text{ km}^2$ late Pleistocene shield volcano and two superimposed late Pleistocene stratovolcanoes: Ushkovsky (or Plosky Dalny, elev. 3,943 m) and Krestovskiy (or Plosky Blizhniy, elev. 4,108 m). Ushkovsky is crowned with two nested calderas which according to Melekestsev et al. (1974) resulted from magma drainage caused by lava venting lower on the slopes.

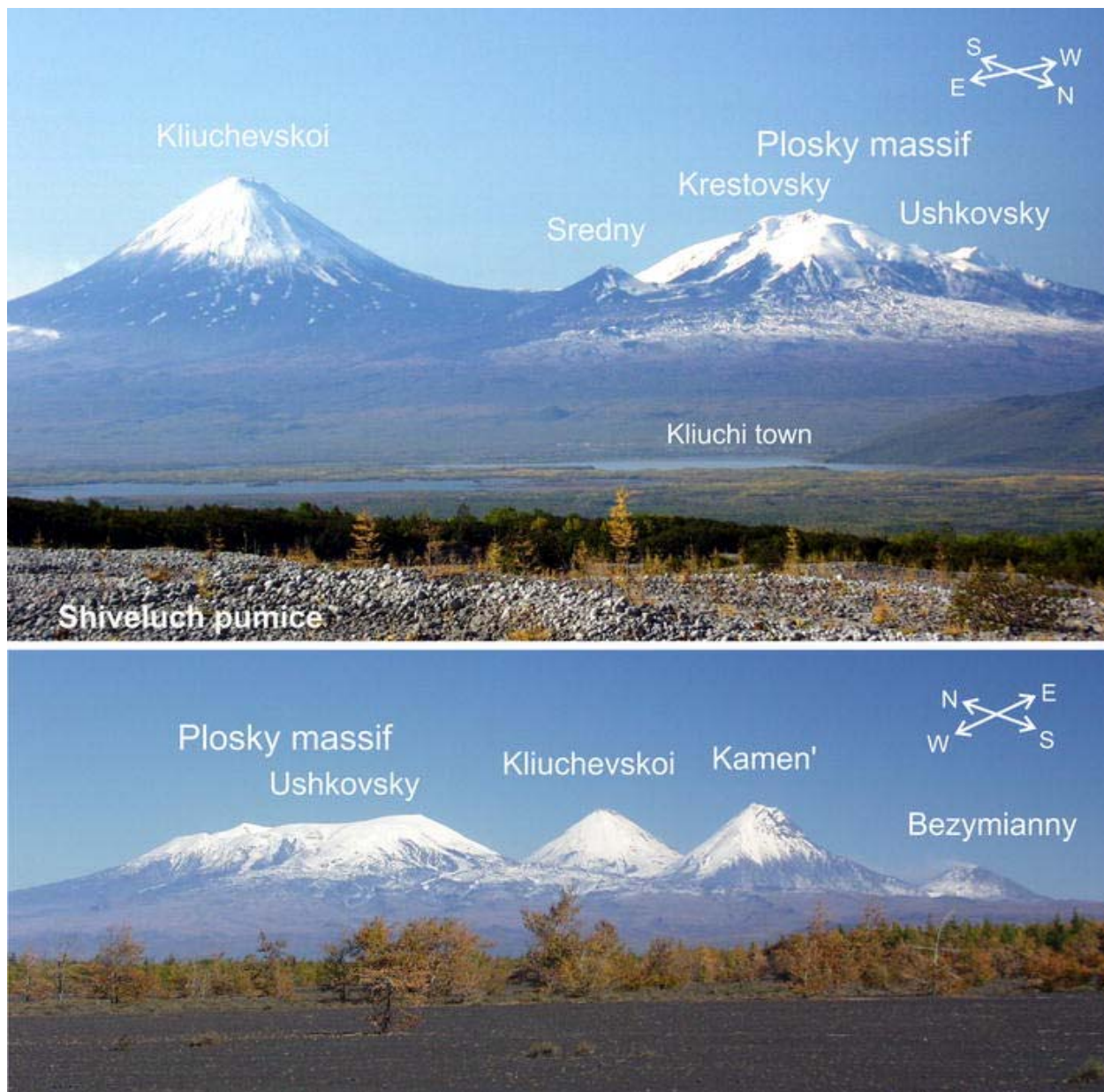


Fig. 2

Panorama photos of the Kliuchevskoi volcanic group including the Plosky volcanic massif, the latter made up by Ushkovskiy (Plosky Dalny) and Krestovskiy (Plosky Blizhniy) volcanoes. *Upper photo* view southward from the slope of Shiveluch volcano; *lower photo* view eastward from along the Kamchatka River valley (see Fig. 1 for orientation). Photos by Philip Kyle

Summit calderas host a glacier which descends down several valleys and partly obscures proximal deposits and flank vents (Fig. 1). Two ice-clad cinder cones with large craters are located in the younger caldera (Flerov and Ovsyannikov 1991; Shiraiwa et al. 2001). An arcuate rift-like zone punctuated by cinder cones crosses the volcanic massif and goes down its SW and NE flanks (Fig. 1; Melekestsev et al. 1974). The zone started to form in late Pleistocene time and continued its activity into the early Holocene. In the northeastern sector of the summit area, near the larger caldera rim, Holocene lavas from this zone and from the intracaldera vents overlie a 40-m-thick cindery tephra (Flerov and Ovsyannikov 1991). Two large Holocene lava flows on the northeastern (Lavovy Shish lava field) and southwestern slopes of the volcanic massif were

the most recent from this zone (Fig. 1).

The younger ~4 km-wide caldera at the summit of Ushkovsky formed roughly 8,600 ¹⁴C years BP as a result of eruptions of lava flows and cinder cones of the Lavovy Shish group (Braitseva et al. 1995). The same events likely triggered the collapse of Krestovsky volcano; its summit likely collapsed as a tephra block, now forming Mt. Sredny (Fig. 2) (Melekestsev 2005), but few data supporting these suggestions have been published. Two early Holocene tephras were attributed to Plosky and used as local markers by Ponomareva et al. (2007b), but no detailed data reported. The magnitude of Plosky explosive eruptions has not been previously estimated, and thus the volcano has not been listed as a source volcano for large Holocene eruptions (Braitseva et al. 1997b; Ponomareva et al. 2007a; Siebert and Simkin 2002).

Plosky activity has been considered to have been mainly effusive with the most recent lavas produced along the rift zone and in the Ushkovsky summit calderas (Flerov and Ovsyannikov 1991). “Active” status has been assigned to Ushkovsky volcano based on weak fumarole activity and presence of thermal spots on its summit (Ovsyannikov et al. 1985). The historic 1890 eruption (Herz 1897) also was likely related to its fumarolic activity (Melekestsev et al. 1991) because no geological evidence of recent explosive activity has been found near its summit (Flerov and Ovsyannikov 1991). Bulk rock analyses permit identification of two groups of Plosky rocks: medium-K and high-K (Churikova et al. 2001). High-K rocks fill the summit calderas and tend to be associated with the rift-like structure, while medium-K lavas belong dominantly to the stratovolcanoes (Flerov and Ovsyannikov 1991).

Materials and methods

Samples

Tephrostratigraphic studies included measuring and sampling of more than thirty tephra sections at Kliuchevskoi, Plosky and Shiveluch slopes (Figs. 1, 3, 4) and tracing Plosky tephra layers from site to site while considering changes in thickness and grain size (Fig. 4). Samples from the western Bering Sea floor were collected from cores SO201-2-77KL and SO201-2-81KL (pilot), obtained in 2009 during the R/V SONNE cruise 201 Leg 2 within the framework of the KALMAR project (Dullo et al. 2009). All samples were washed with distilled water. Submarine sample SO201-77-SR1 was sieved to obtain three fractions (>0.1, 0.1–0.05, and <0.05 mm).

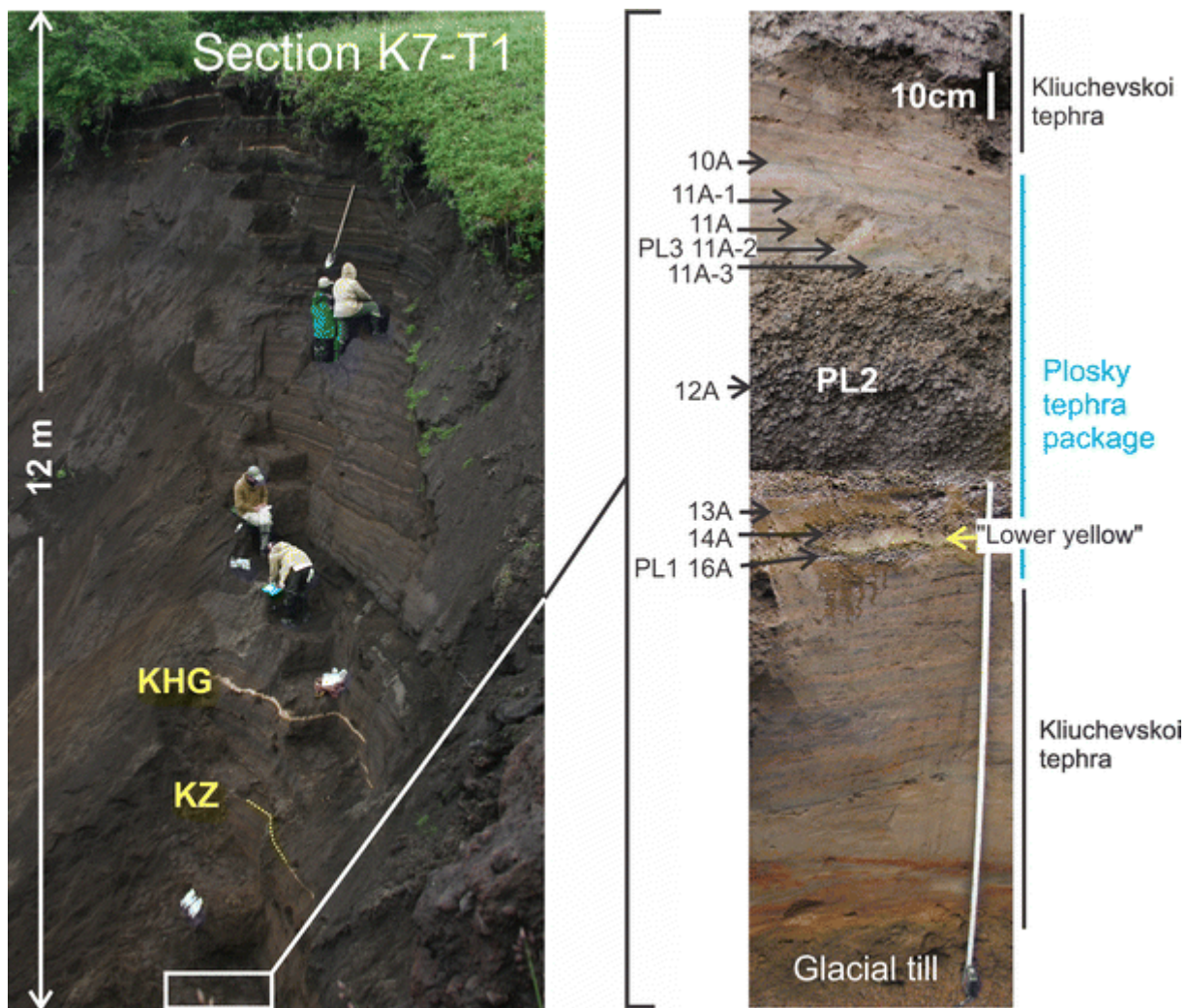


Fig. 3

Left photo of section K7-T1 (Fig. 1) through a ~12-m-thick Holocene tephra sequence on the slope of Kliuchevskoi volcano. Right photo detail with the Plosky tephra package. The sequence is dominated by *dark-gray cinders* from Kliuchevskoi volcano interbedded with ~30 *light-colored tephra layers* from other volcanoes (Portnyagin and Ponomareva 2012). Plosky package lies close to the bottom of the Holocene tephra sequence and in this area includes 2–4 cinder lapilli layers and a few tephra layers of fine to very fine sand size. The lowermost lapilli layer is separated from the upper layers by a sandy loam with intercalated *yellow pumiceous tephra* ("lower yellow"). Analyzed Plosky samples are shown with *arrows*; full sample ID consists of section ID (K7-T1) followed with the sample number. Regional marker tephra layers: KHG (Khangar volcano, ~7,800 cal BP, Bazanova and Pevzner 2001) and KZ (Kizimen volcano, ~8,250 cal BP, Braitseva et al. 1997b). Photo at the left courtesy A. Plechova

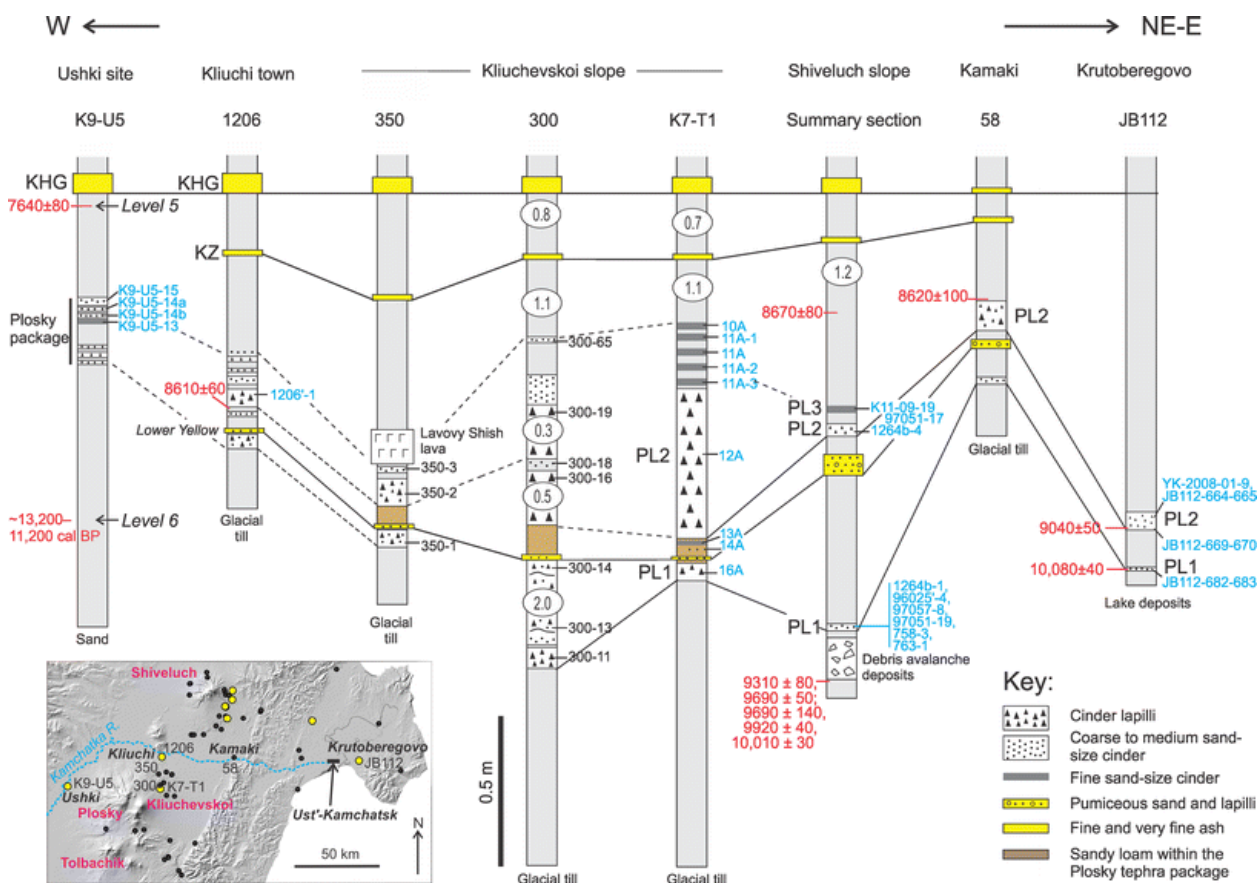


Fig. 4

Graphic measured sections at selected terrestrial sites (*inset*) from the Khangar marker tephra (KHG) down through the early Holocene Plosky tephra package; only details of Plosky and major marker tephras are shown. Sediments interlayered with Plosky layers are represented by sandy loams, peat, and other tephras, the latter dominantly from Kliuchevskoi and Shiveluch; proximity to these volcanoes can dramatically alter the total-package thickness. Where the sections are graphically compressed, true thickness is shown in *meters*, within *ovals*. Analyzed samples' IDs are provided right to each *column* (*black font* for bulk tephra, *blue* for glass analyses), and full sample ID is given except for K7-T1 where "K7-T1" is the official prefix for each of these samples. Radiocarbon dates (*left side of column*) are from Goebel et al. (2003), Braitseva et al. (1988, 1995), Ponomareva et al. (2007b), Pevzner et al. (2012), and this study. Regional marker tephra layers: KHG (Khangar volcano, ~7,800 cal BP, Bazanova and Pevzner 2001) and KZ (Kizimen volcano, ~8,250 cal BP, Braitseva et al. 1997b). Archaeological levels 5 and 6 in Ushki from Dikov (2003)

Geochemistry

Major elements in bulk cinder samples were determined by wet chemistry in the Institute of Volcanology and Seismology (Petropavlovsk-Kamchatsky, Russia). Lava sample from Lavovy Shish lava field was analyzed by XRF in GEOMAR (Kiel). Volcanic glass and minerals were analyzed using a JEOL JXA 8200 electron microprobe equipped with five wavelength dispersive spectrometers including 3 high-sensitivity ones (2 PETH and TAPH) at GEOMAR (Kiel). The analytical conditions for glasses were 15 kV accelerating voltage, 6 nA current, and 5 μm electron beam size. The details of the settings and standards used and of data reduction can be found in Online Resource 1. The INTAV intercomparison of electron beam microanalysis of glass by tephrochronology laboratories (Kuehn et al. 2011) revealed no systematic error for glass compositions analyzed at GEOMAR lab (coded as lab #12).

Trace elements in glasses were analyzed by laser ablation—inductively coupled plasma—mass spectrometry (LA-ICP-MS) using a 193-nm excimer laser with a large volume ablation cell (Zürich, Switzerland) coupled with a quadrupole-based ICP-MS (Agilent 7500cs) at the Institute of Geosciences, CAU Kiel, Germany. In situ-microsampling was done with 50- μm pit size. The details of the settings used can be found in Online Resource 1.

Dating

The ages of the two major tephra layers (PL1 and PL2) from Plosky were obtained through AMS ^{14}C dating on pollen and leaf fragments collected from inside each tephra in a $\sim 7\text{-m}$ -deep peat section (JB112) near Krutoberegovo village (Fig. 4). AMS radiocarbon analysis was performed by Beta Analytic. Quoted errors represent one relative standard deviation statistics (68 % probability). Radiocarbon ages were corrected for isotopic fractionation and were calibrated using the IntCal09 curve (Reimer et al. 2009). Calibrated ranges are reported as two standard deviations. For approximate age estimates of other events, we use calibrated ^{14}C ages except for the cases where we cite other authors' published dates.

Results

Proximal tephra and lava sequence

Cinder lapilli attributed to Plosky based on similarity of their bulk composition to high-K andesitic Plosky lavas were documented in many outcrops on the slopes of Kliuchevskoi volcano (Figs. 1, 3, 4; Auer et al. 2009). In this area, a 10–12-m-thick Holocene tephra sequence is dominated by numerous dark-gray cinders from Kliuchevskoi, interbedded with ~ 30 light-colored tephra layers from other volcanoes (Portnyagin and Ponomareva 2012). Plosky lapilli lie in the lower part of the sequence, well below a regional marker tephra layer (KZ) dated at $\sim 8,250$ cal BP (Braitseva et al. 1997a; Auer et al. 2009) (Fig. 3).

A series of lava flows similar in bulk composition to the described Plosky cinders and to high-K andesitic Plosky lavas (Churikova et al. 2001) are associated with several vents on the Plosky slopes. Lava flows on the northeastern slope, usually referred to as Lavovy Shish lava field (Fig. 1), directly overlie the Plosky lapilli and likely close this eruptive episode. At high elevations, where lava is not covered by younger deposits, it bears features typical for low-viscosity lavas, such as remnants of lava tubes and fragments of undulating or ropy surfaces. The lava is porphyric trachyandesite (Table 1) with plagioclase crystals up to 1 cm long referred to by Piip (1956) as mega-plagiophyric. Closer to Plosky, Lavovy Shish lavas are partly covered by a glacier and, in their terminal part, they are obscured by a younger debris fan from Kliuchevskoi volcano; hence, their real extent is not known. The stratigraphic position of the lava flow on the southwestern slope is less clear because the tephra cover is less stable at

elevations >1,100 m. However, this lava likely formed in early Holocene because it overlies Last Glacial Maximum moraines and is in turn overlain by KHG marker tephra dated at ~7,800 cal BP (Braitseva et al. 1997a). Because this lava flow is located within the same rift-like zone as the northeastern lava field and is close to the latter in surface morphology, petrography, and age, we include it in the same eruptive episode.

Table 1

Major element composition of Plosky tephra and lava

Sample#	Site location	Tephra code	SiO ₂	TiO ₂	Al ₂ O ₃	Fe ₂ O ₃	FeO	MnC
300-19	Kliuchevskoi volcano		56.05	1.35	17.59	3.20	4.99	0.19
300-18	Kliuchevskoi volcano		56.53	1.33	17.63	2.02	5.35	0.15
300-18 duplicate	Kliuchevskoi volcano		56.90	1.32	17.30	3.51	4.28	0.17
300-16	Kliuchevskoi volcano	PL2	56.47	1.34	17.34	2.88	4.87	0.18
300-14	Kliuchevskoi volcano		58.40	0.95	17.13	3.60	4.18	0.16
300-13	Kliuchevskoi volcano		58.54	0.98	17.49	3.67	4.03	0.16
300-11	Kliuchevskoi volcano	PL1	58.34	1.03	17.47	3.64	3.84	0.15
350-3	Kliuchevskoi volcano		56.42	0.99	20.51	3.00	4.54	0.17
350-2	Kliuchevskoi volcano		56.43	1.08	19.35	4.04	4.34	0.19
350-1	Kliuchevskoi volcano	PL1	56.64	1.07	18.96	3.51	4.69	0.17
1206'-1	Kliuchi town		56.81	1.24	19.91	2.99	4.03	0.10
K8-39 (lava)	Kliuchevskoi volcano	Lavovy Shish	57.48	1.01	20.08		5.46*	0.09

All analyses except for the last one were performed by wet chemistry method in the Institute of Volcanology, Petropavlovsk-Kamchatsky, Russia. Sample K8-39 was analyzed by XRF in GEOMAR (Kiel). * Total Fe as FeO

In all sections on Kliuchevskoi slopes, Plosky cinders form a package (“Plosky package”) of two to four lapilli layers interlayered and topped with a few layers of finer grained sand-sized tephra (Figs. 3, 4). The lower lapilli layers are separated from upper layers by a 6–10-cm-thick sandy loam, which signifies a break in Plosky’s explosive activity and contains a 1–2-cm-thick layer of

bright-yellow pumiceous tephra dubbed “lower yellow”. In section 300, one of the lower lapilli layers is >2 m thick and probably is related to one of the cinder cones (Fig. 4). This layer pinches out laterally, unlike other two lapilli layers that can be traced over a large area and likely came from the summit crater. Maximum lapilli size is 10 cm from sample 300–16 (Fig. 4).

Continuous sampling of a section through the tephra sequence (K7-T1 on Figs. 1, 3, 4) and new analyses of bulk cinders and their glass allowed us to geochemically characterize dominant Kliuchevskoi cinders (Portnyagin et al. 2009) and to single out nine individual tephra layers compositionally close to known high-K Plosky rocks (Krasheninnikov 2008; Figs. 3, 4). Glass from all these layers, and minerals from three layers, were analyzed with an electron microprobe (EMP). Glass from the thickest lapilli layer (sample K7-T1-12A) was analyzed by LA-ICP-MS. In addition, we used bulk rock analyses from this section and sections 300, 350 and 1,206 (Figs. 1, 4; Table 1) (Auer et al. 2009, and this study).

Plosky tephra comprises vesicular dark-gray porphyric cinders with vitric groundmass (Figs. 5, 6) containing very rare microlites. Many glass particles have a sponge-like texture with highly elongated vesicles. The mineral assemblage is dominated by large, elongated (≤ 1 cm long) plagioclase phenocrysts (An_{44-78} , $K_2O = 0.2-1.1$ wt%, $FeO = 0.42-0.88$ wt%) which are typically normally zoned with the exception of sample K7-T1-16A, where plagioclase phenocrysts exhibit a weak reverse zoning. Rare subphenocrysts and microlites include olivine ($Fe_{0.71-0.72}$) in sample K7-T1-12A, clinopyroxene ($Mg\# = 69-76$ mol %, $CaO = 17-19.5$ wt%, $TiO_2 = 0.51-0.77$ wt%, $Al_2O_3 = 1.79-2.85$ wt%, $Na_2O = 0.22-0.41$ wt%), low-Ca pyroxene ($Mg\# = 66-75$ mol %, $CaO = 1.6-2.1$ wt%, $TiO_2 = 0.25-0.46$ wt%, $Al_2O_3 = 0.77-1.94$ wt%, $Na_2O = 0.01-0.10$ wt%), and Ti-magnetite ($TiO_2 = 8-19$ wt%, $Al_2O_3 = 2.2-5$ wt%) (Online Resource 2). Rare F–Cl apatite grains have been found in sample K7-T1-14A.

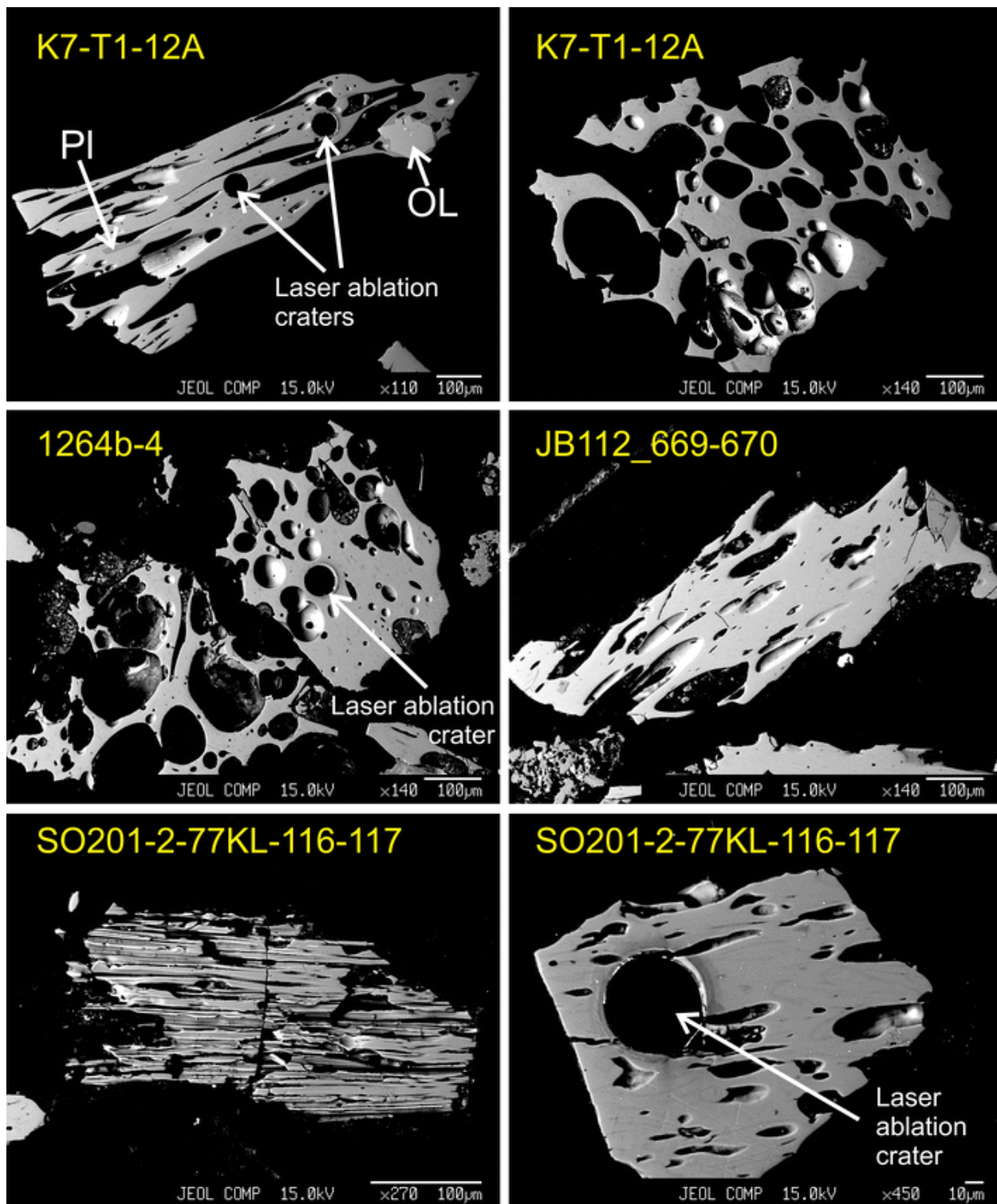


Fig. 5

Backscattered electron images of analyzed PL2 tephra collected in different sites from proximal (*top*) to distal marine (*bottom*). Labeled mineral phases: *Ol* olivine, *Pl* plagioclase. Terrestrial samples: K7-T1-12A (23 km from source), 1264b-4 (78 km), JB112-669-670 (140 km). Marine sample SO201-2-77KL-116-117 is 635 km from the source. Sample numbers correspond to those in Figs. 3 and 4, Tables 2, 3 and 4, and Online Resources 2 and 3

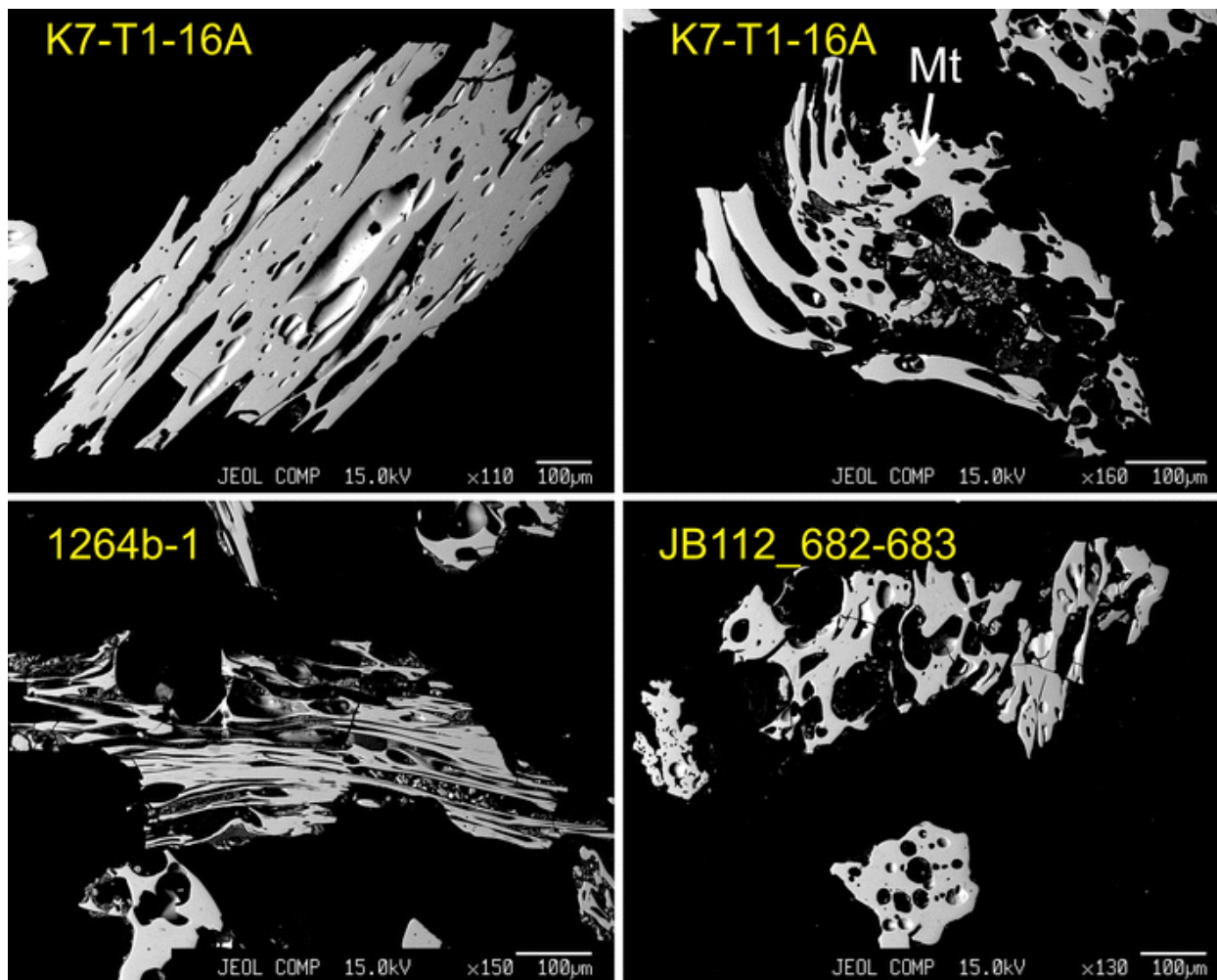


Fig. 6

Backscattered electron images of analyzed PL1 tephra collected from the same terrestrial localities as shown in Fig. 5. Sample numbers correspond to those in Figs. 3 and 4, Tables 2, 3 and 4, and Online Resources 2 and 3

All tephra consist of fresh magmatic particles, with only a minor amount of recrystallized rock fragments. SiO_2 content in bulk cinder lapilli varies from 56 to 58.5 % (Fig. 7). Glass from all the cinders forms a trend in the trachyandesitic–trachydacitic field with SiO_2 ranging from 58 to 64.5 wt% (Fig. 7; Online Resource 3). Classification diagrams show that Plosky cinders have intermediate compositions between medium-K basaltic andesites, andesites, and high-K basaltic trachyandesites–trachyandesites (Fig. 7; Table 1) and are different from Kliuchevskoi medium-K basalts–basaltic andesites of normal alkalinity (Fig. 7). On the SiO_2 – FeO/MgO diagram, most Plosky bulk rock and glass compositions fall into the tholeiitic and medium-Fe fields (Fig. 7).

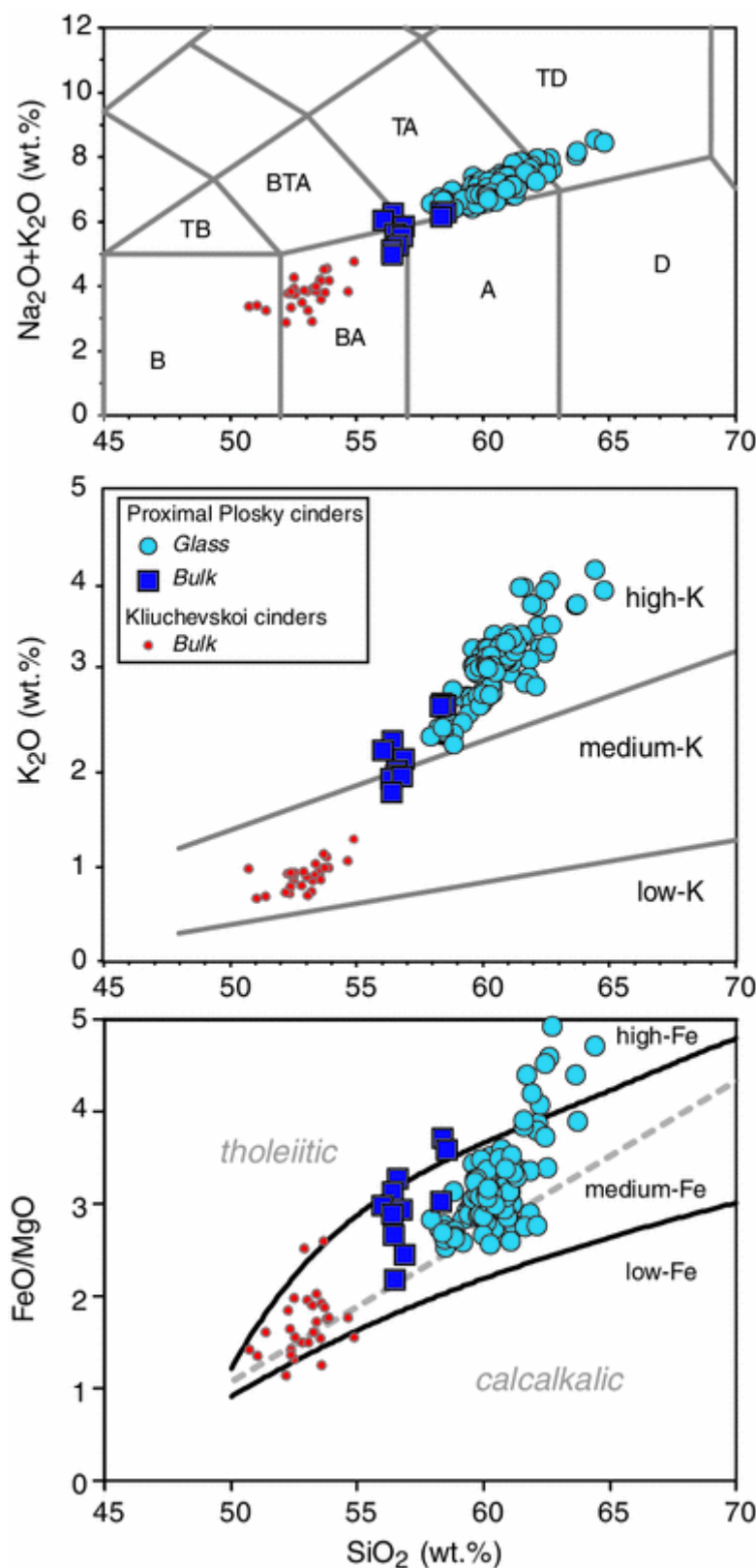


Fig. 7

Classification diagrams for proximal Plosky (glass and bulk) and Kliuchevskoi (bulk) cinders. In the TAS diagram (*top*), fields are according to Le Bas et al. (1986): B basalt, BA basaltic andesite, A andesite, D dacite, TB trachybasalt, BTA basaltic trachyandesite, TA trachyandesite, TD trachydacite. In the SiO_2 versus K_2O diagram (*middle*), the fields of low-, medium-, and high-K rocks are according to Gill (1981). In the SiO_2 versus FeO/MgO diagram (*bottom*) tholeiitic and calc-alkalic series after Miyashiro (1974), and low-, medium- and high-Fe series after Arculus (2003). FeO in bulk samples refers to total Fe expressed as FeO

The majority of Plosky glasses have $\text{SiO}_2 = 59\text{--}61$ wt%, $\text{K}_2\text{O} = 2.5\text{--}3.5$ wt%, and $\text{MgO} = 2\text{--}2.7$ wt% (Fig. 7; Table 2). One lapilli tephra (K7-T1-12A), which forms the thickest layer in the K7-T1 section (Figs. 3, 4), clearly stands apart and has the most mafic glass in the package with $\text{SiO}_2 = 58\text{--}59.2$ wt%, $\text{K}_2\text{O} = 2.3\text{--}2.5$ wt%, and $\text{MgO} = 2.8\text{--}3$ wt% (Figs. 8, 9). Glasses from two tephra (K7-T1-11A and K7-T1-11A-3; Figs. 3, 4) have the most fractionated silicic, high-K, and low-Mg glass compositions (Fig. 8). Temporal variations of glass compositions are irregular except for those for chlorine whose concentrations in glass correlate significantly ($r^2 = 0.55$) with stratigraphic position of samples (Fig. 8; Table 2). The concentrations of Cl do not correlate with any other element in Plosky glasses and increase progressively from about 0.03 ± 0.01 wt% (± 1 sd) in the oldest samples to about 0.05 ± 0.01 wt% in the youngest ones. This characteristic may be used to discriminate Plosky glasses of different ages.

Table 2

Average electron probe analyses of volcanic glass from proximal Plosky tephras

Sample# Eruption ID Grain size Age (cal BP) N anls	K7-T1-10A Fine to very fine ash <10,200 14		K7-T1-11A-1 Fine to very fine ash <10,200 7		K7-T1-11A Fine to very fine ash <10,200 11		K7-T1-11A-2 PL3 Fine to very fine ash <10,200 10	
	Average	1 sd	Average	1 sd	Average	1 sd	Average	1 sd
SiO ₂	59.80	0.47	59.95	0.59	62.27	0.83	60.37	0.51
TiO ₂	1.60	0.06	1.64	0.07	1.69	0.09	1.53	0.04
Al ₂ O ₃	15.23	0.32	14.93	0.47	14.30	0.44	15.49	0.12
FeO	7.65	0.30	7.63	0.57	7.12	0.58	7.13	0.51
MnO	0.16	0.05	0.16	0.04	0.12	0.04	0.09	0.04
MgO	2.57	0.14	2.50	0.11	1.71	0.27	2.50	0.14
CaO	5.42	0.25	5.32	0.31	4.17	0.37	5.07	0.28
Na ₂ O	3.94	0.16	3.85	0.09	4.02	0.17	4.10	0.25
K ₂ O	2.84	0.16	3.15	0.24	3.73	0.28	2.94	0.18
P ₂ O ₅	0.68	0.05	0.76	0.08	0.75	0.09	0.69	0.04
Cl	0.06	0.01	0.05	0.01	0.06	0.01	0.05	0.01
F	0.04	0.04	0.04	0.06	0.05	0.05	0.02	0.03
SO ₃	0.02	0.02	0.02	0.02	0.01	0.01	0.01	0.01
Total	100		100		100		100	

All samples are from K7-T1 section located 23 km northeast of Plosky volcano (Fig. 3). All analyses are normalized on anhydrous basis. Analyses of individual glass shards are presented in Supplementary table 1

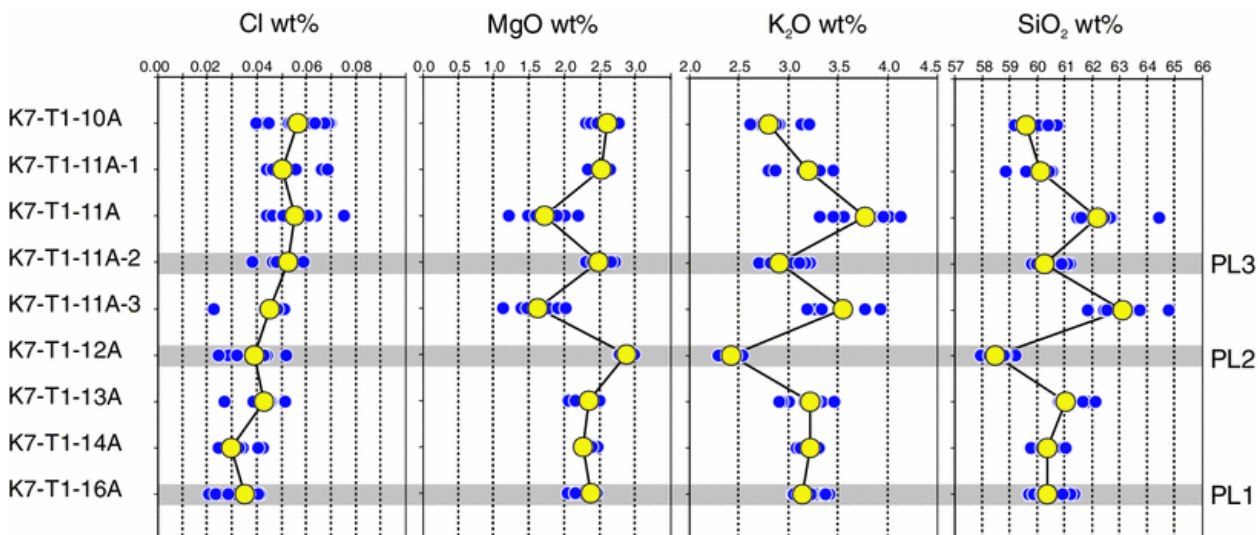


Fig. 8

Graph of temporal variations in composition of glasses from individual Plosky tephra layers, in stratigraphic order from excavation K7-T1 (Figs. 3, 4). *Small symbols* denote individual glass-shard analyses; *large circles* are sample averages. The three major Plosky tephras discussed in this paper are indicated by *gray bars*

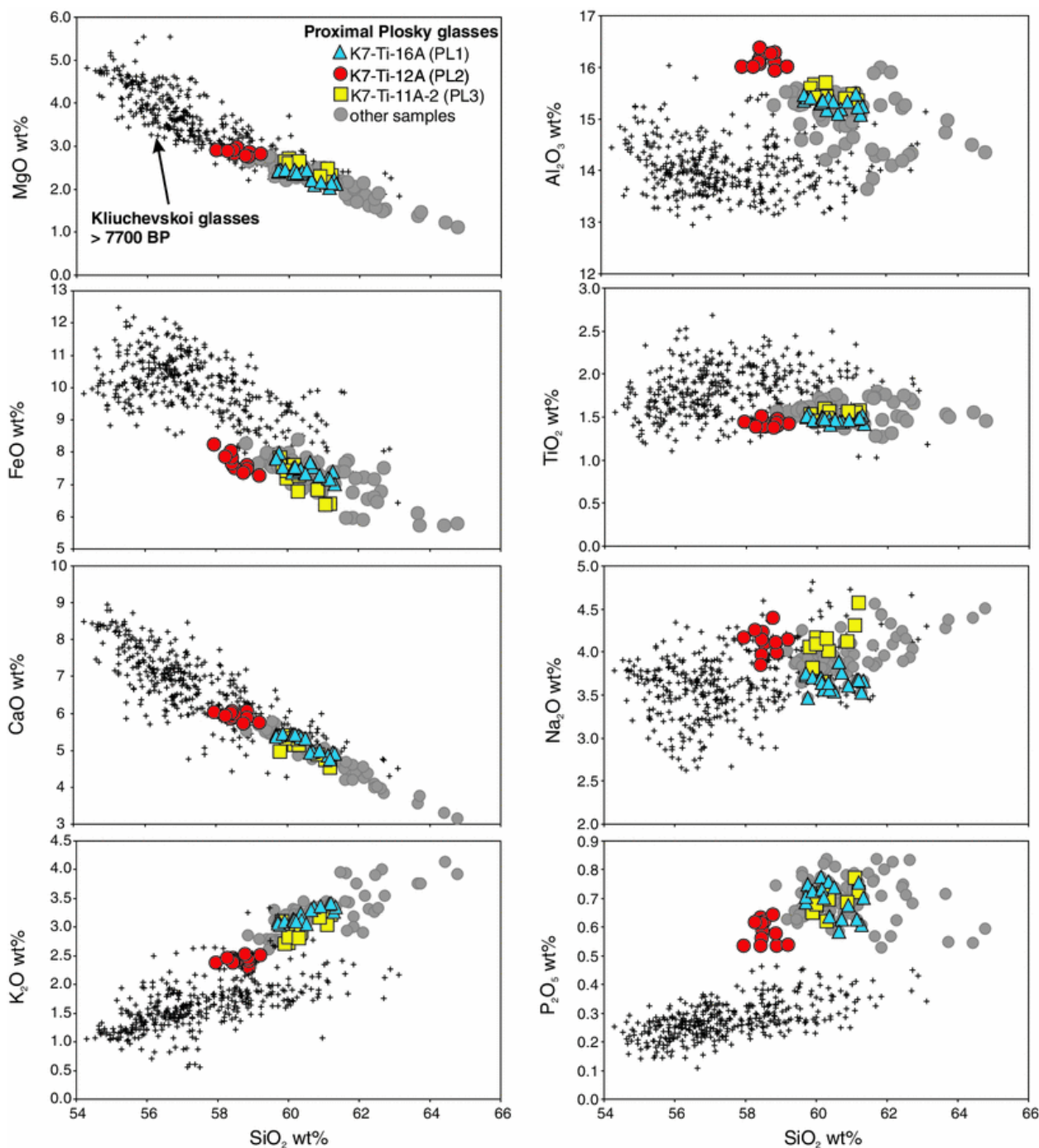


Fig. 9

Graphs of major element composition of glasses from proximal Plosky tephra deposits. Glasses from Kliuchevskoi tephra older than 7,700 cal BP are shown for comparison (Krasheninnikov 2008; M. Portnyagin and V. Ponomareva, unpublished data)

Compared to glasses from Kliuchevskoi cinders (Fig. 9), Plosky glasses tend to have more silicic, exclusively trachyandesitic compositions. In the field of andesitic compositions, Plosky glasses have lower FeO and TiO₂ and higher Al₂O₃, K₂O and P₂O₅ compared to the most evolved Kliuchevskoi glasses. Concentrations of phosphorous provide particularly useful criteria for reliable discrimination of Plosky and Kliuchevskoi glasses. All Plosky glasses have concentrations of P₂O₅ > 0.5 wt%, whereas those from Kliuchevskoi have P₂O₅ < 0.5 wt%.

Trace element data obtained for Plosky cinder K7-T1-12A include bulk rock analysis (high-

precision XRF on pressed tablets, Auer et al. 2009) and LA-ICP-MS data on single glass shards (Table 3, this study). The data are compared with each other and with published compositions of lavas from Plosky and Kliuchevskoi volcanoes in Fig. 10. The compositions of bulk rock and glass for Plosky lapilli sample K7-T1-12A are similar. Approximately 10 rel. % lower concentrations of incompatible elements in bulk rock analyses (Rb, Ba, Nb, La, Pb, Zr, Y) indicate the presence of Sr-rich plagioclase phenocrysts (~10 %) in the bulk rock. Both bulk tephra and glasses show a typical pattern for evolved Kamchatka magma formed in subduction-related environments (e.g., Gill 1981). The compositions are enriched in all REE ($\geq 10\times$ mantle values), moderately enriched in light REE (LREE) over heavy REE (La/Yb ~ 5.3), strongly enriched in Pb, U and large-ion lithophile elements (LILE) (Ba, Rb, Cs), and depleted in Nb and Ta relative to LREE (e.g., $Pb_N/Ce_N = 4.3$, $Ba_N/La_N = 3.2$, $Nb_N/La_N = 0.27$ in glasses, where N refers to mantle-normalized values). The pattern of LILE (Cs, Rb, Ba) and U is unfractionated, while the ratios of these elements are similar to those in primitive mantle (i.e., $Ba_N/Rb_N \sim 1$, $Rb_N/U_N \sim 1$, etc., Fig. 10).

Table 3

Major and trace element concentrations in single tephra glass shards and reference glasses obtained by LA-ICP-MS

Sample	Units	K7-T1-12A		YK-2008-01-9		1264b-4		SO201
Eruption/layer ID		PL2		PL2		PL2		PL2/S]
Elements		Mean (<i>n</i> = 5)	SD	Mean (<i>n</i> = 5)	SD	Mean (<i>n</i> = 4)	SD	Mean (<i>n</i> = 4)
SiO ₂	wt%	62.3	1.1	63.8	1.9	66.2	0.8	58.9
CaO	wt%	5.95	0.00	5.98	0.13	6.24	0.03	5.61
Li	ppm	27.1	0.7	28.0	0.8	28.8	1.0	26.5
Sc	ppm	23.5	0.2	24.3	0.8	24.5	0.7	22.2
Ti	ppm	8,118	114	8,363	429	8,350	197	7,655
V	ppm	252	5	258	10	259	10	241
Cu	ppm	179	4	172	36	202	14	180
Zn	ppm	104	7	107	4	132	16	104
Ga	ppm	21.8	0.8	23.9	1.9	25.2	1.7	21.6
As	ppm	6.69	0.41	7.27	0.91	7.32	0.33	6.43
Rb	ppm	79.2	2.5	81.1	1.9	84.0	4.7	77.5
Sr	ppm	297	7	302	7	321	5	286
Y	ppm	47.9	0.7	49.1	1.2	51.0	1.7	45.2
Zr	ppm	331	7	358	21	359	12	313
Nb	ppm	6.97	0.21	7.46	0.35	7.53	0.16	6.64
Mo	ppm	3.70	0.13	3.81	0.13	3.99	0.29	3.54
Sb	ppm	0.96	0.04	1.03	0.06	1.10	0.03	0.94
Cs	ppm	2.85	0.06	2.96	0.10	2.97	0.15	2.71

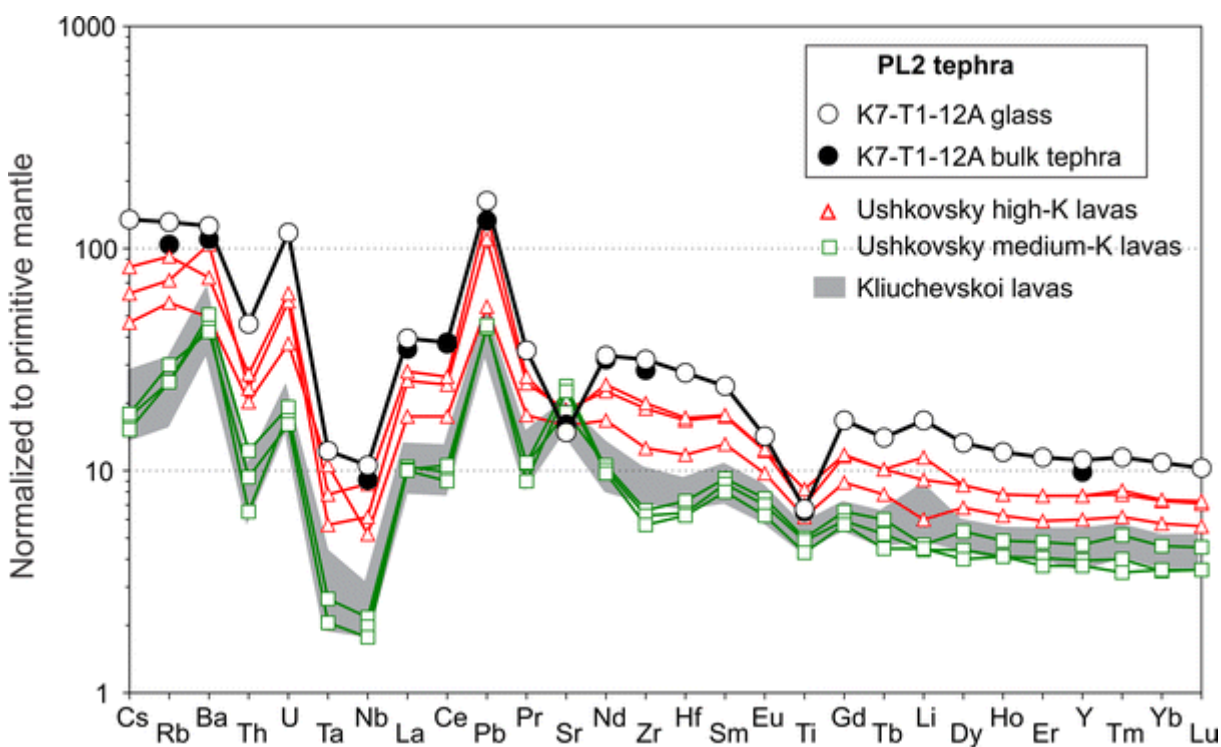


Fig. 10

Plot of trace element composition of proximal Plosky tephra PL2 (sample K7-T1-12A) normalized to primitive mantle (McDonough and Sun 1995). Bulk analyses (*closed circles*) are from Auer et al. (2009); average LA-ICP-MS glass analyses (*open circles*) are from this study. The composition of high-K and middle-K Ushkovsky lavas and Kliuchevskoi lavas after Churikova et al. (2001)

The pattern of trace elements in the tephra is subparallel to those of high-K basaltic and basaltic andesitic Plosky lavas, which suggests a possible genetic link between these magmas by fractional crystallization from a common parental magma. Lower Sr and Ti concentrations and a more pronounced negative Eu anomaly in the andesitic glass, compared to the high-K Plosky lavas, imply that the fractional crystallization involved plagioclase (a major host for Sr and Eu) and Fe–Ti oxides (hosts for Ti) along with Fe–Mg silicates (olivine and pyroxenes) in good agreement with the petrographic observations. Middle-K lavas from Plosky and Kliuchevskoi volcano have distinctively lower concentrations of most incompatible elements and exhibit a characteristic Ba enrichment relative to similarly incompatible trace elements (e.g., $Ba_N/Rb_N \sim 2$ in Kliuchevskoi and middle-K Plosky lavas). This observation indicates that the high-K and middle-K series of Plosky volcanic massif originated from different parental magmas.

Overall, the geochemical characteristics of Plosky tephra make it quite a rare type of Holocene volcanic composition in Kamchatka, resembling to a certain extent only the most evolved lavas of Gorely volcano (Duggen et al. 2007). This specific composition facilitates identification of this tephra in distal localities.

Distal tephra sections

Terrestrial sections

The Plosky tephra package was directly traced from section to section northeast of the source, to the southern and eastern slopes of Shiveluch volcano, and farther east toward Ust'-Kamchatsk and Krutoberegovo villages over the distance of ~150 km (Figs. 4, 11b). In all these distal sections, it consists of three layers of black or brownish-black cinders, from bottom to top—fine tephra overlain by medium-to-coarse tephra overlain by very fine tephra (Fig. 12). Because of their dark color, Plosky tephra layers are visible among light-colored, pumiceous Shiveluch tephra and are good markers for Shiveluch sections. The direction from Plosky volcano toward Shiveluch sites goes close to K7-T1 section (Fig. 11b), where we have geochemically characterized the Plosky tephra package in detail. Therefore, all three Plosky tephra found at Shiveluch and farther east must be present in section K7-T1.

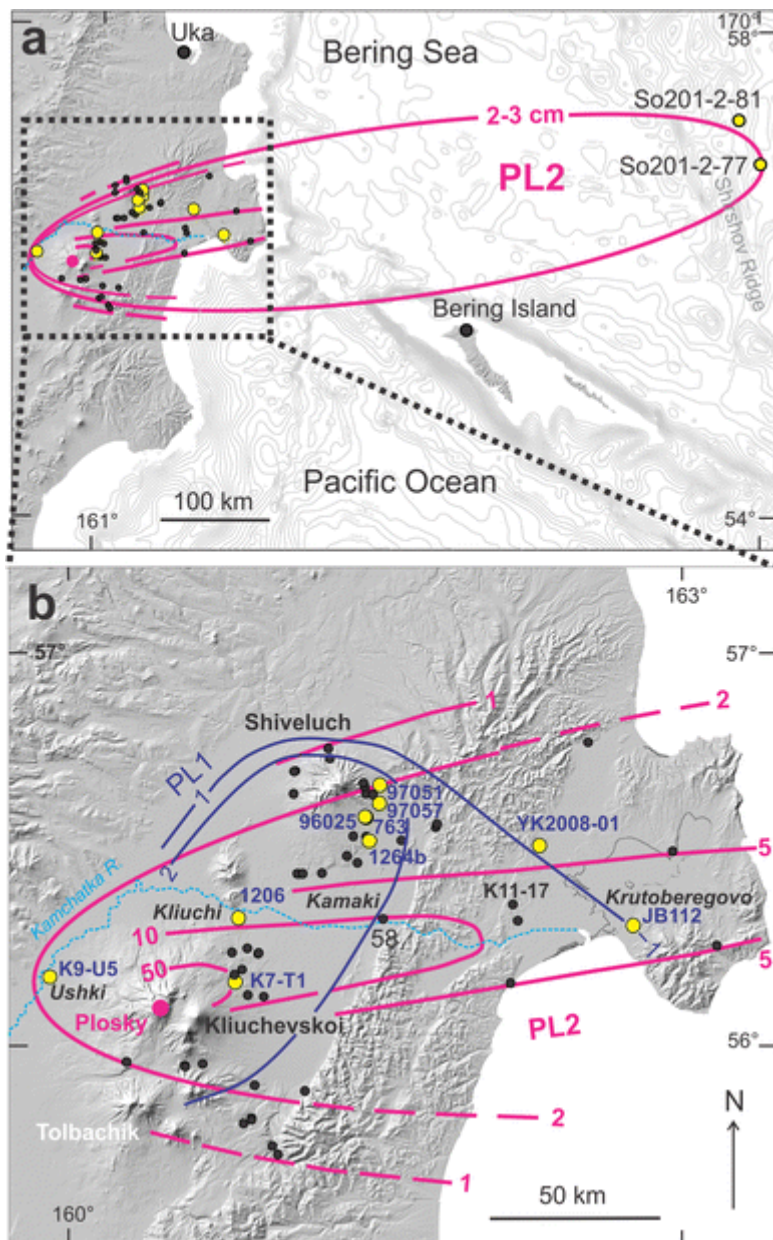


Fig. 11

Maps of dispersal of Plosky tephras. **a** Approximate position of a 2.5 cm isopach for PL2 tephra. Sites at Uka and on Bering Island are peat sections where no Plosky tephra has been found. **b** *Enlarged inset* from **a** showing isopach lines for PL2 (*magenta*) and PL1 (*dark-purple*); thickness in cm. Other symbols as in Fig. 1

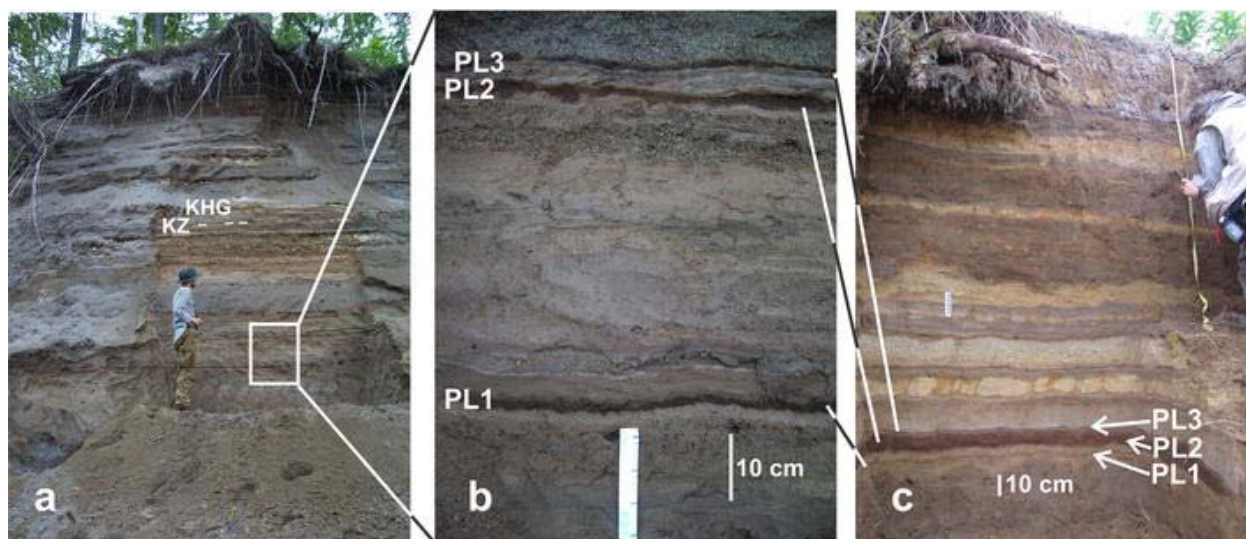


Fig. 12

Photos of Plosky tephra package interlayered with Shiveluch tephra, **a**, **b** at the southeastern slope of Shiveluch volcano, Kabeku River, site 1264b, 78 km NE from the source (Fig. 11b), and **c** farther east, site K11-17, 107 km ENE from the source (located on Fig. 11b)

Appearance of glass shards from the cindery tephra layers found on Shiveluch slopes (Figs. 5, 6) is similar to that from Plosky tephras. Microprobe analyses of glass from selected samples (Fig. 4) allow us to correlate these three tephra layers to the layers found in section K7-T1 (Fig. 13, Online Resource 3). The lower layer correlates with the lower lapilli tephra K7-T1-16A and the middle layer to the most mafic lapilli tephra K7-T1-12A. Glasses from the upper very fine tephra are close to those in K7-11A-2 fine tephra in section K7-T1. At similar SiO_2 content, glasses from this upper tephra have slightly lower TiO_2 , FeO , and MnO content compared to samples of similar age in the Plosky package in K7-T1 section (K7-10A, K7-11A-1; Tables 2, 4). To confirm the correlation of the most mafic Plosky tephra (K7-T1-12A) with the distant terrestrial samples, trace elements were obtained by LA-ICP-MS for this (most mafic) tephra from the sites K7-T1 (Kliuchevskoi slope), 1264b (Shiveluch), and YK-2008-01 (Ust'-Kamchatsk area) (Figs. 4, 14). The concentrations of trace elements in all three samples are indistinguishable within 15 rel. % and confirm the origin of these tephra layers from the same eruption.

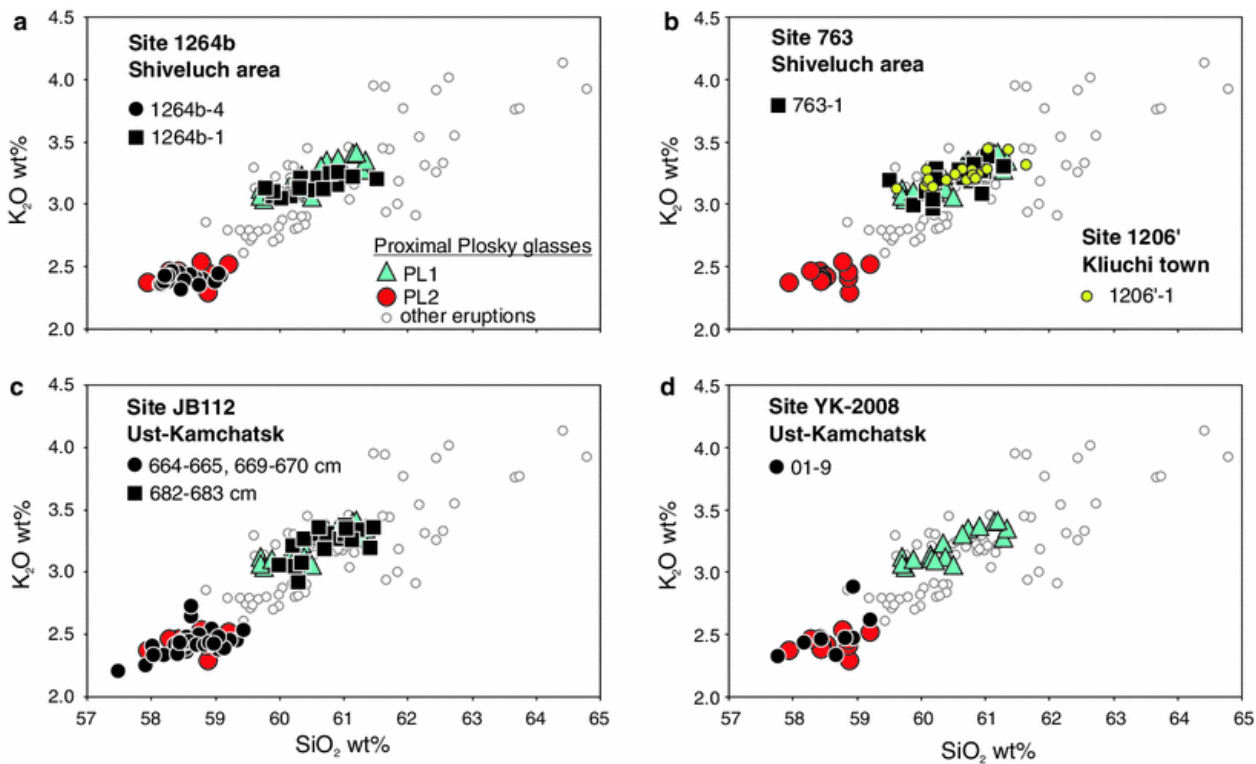


Fig. 13

Graphic plots of composition of tephra glasses from different distal terrestrial sections correlated with proximal Plosky tephras. Sites are located on Fig. 11

Table 4

Average electron probe analyses of volcanic glass from distal Plosky tephtras

Sample# Eruption/layer ID Age (cal BP) LAT/LONG Section location N anls.	1264b-1 PL1 11,650 N 56.5061°E 161.4784° Shiveluch volcano 20		763-1 PL1 11,650 N 56.5671°E 161.4770° Shiveluch volcano 20		97057-8 PL1 11,650 N 56.6322°E 161.4608° Shiveluch volcano 13		97051-19 PL1 11,650 N 56.6572°E 161.4969° Shiveluch volcano 13	
	Average	1 sd	Average	1 sd	Average	1 sd	Average	
SiO ₂	60.40	0.47	60.65	0.45	60.51	0.39	60.29	
TiO ₂	1.52	0.04	1.50	0.03	1.48	0.03	1.48	
Al ₂ O ₃	15.26	0.15	15.16	0.18	15.22	0.12	15.17	
FeO	7.47	0.23	7.42	0.19	7.36	0.32	7.59	
MnO	0.14	0.04	0.14	0.05	0.15	0.05	0.14	
MgO	2.31	0.10	2.24	0.10	2.30	0.10	2.39	
CaO	5.36	0.16	5.22	0.19	5.15	0.15	5.25	
Na ₂ O	3.59	0.12	3.67	0.15	3.83	0.08	3.76	
K ₂ O	3.14	0.07	3.22	0.10	3.17	0.09	3.14	
P ₂ O ₅	0.73	0.05	0.71	0.06	0.71	0.05	0.70	
Cl	0.04	0.01	0.03	0.01	0.03	0.01	0.04	
F	0.04	0.03	0.03	0.03	0.06	0.05	0.03	
SO ₃	0.02	0.02	0.02	0.02	0.02	0.01	0.02	
Total	100		100		100		100	
Sample# Eruption/layer	1264b-4 PL2 10,200		YK-2008-01-9 PL2 10,200		JB112_664–665 PL2 10,200		SO201-2-81_ PL2/SR1 10,200	

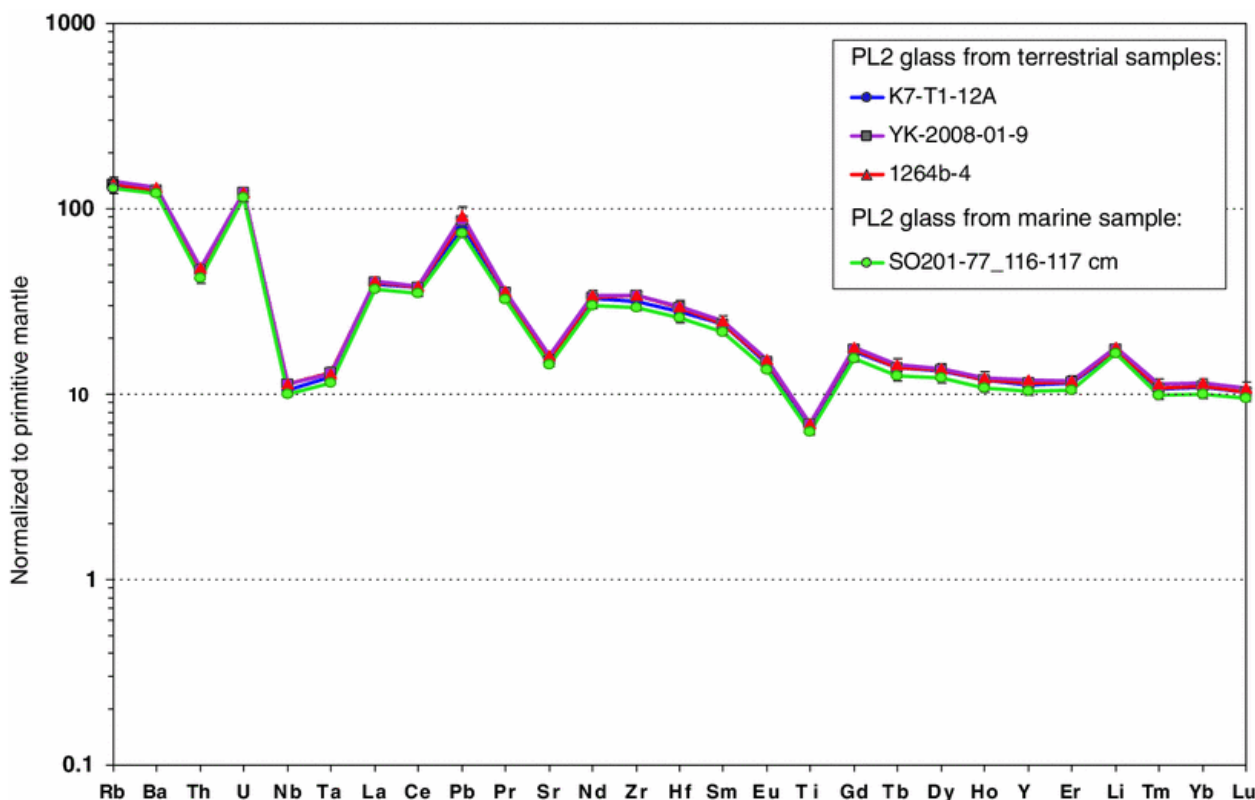


Fig. 14

Plot of trace element composition of volcanic glass from PL2 tephra sampled in terrestrial and marine sections, normalized to primitive mantle (McDonough and Sun 1995). Sample sites are located on Fig. 11

Given the wide spatial dispersal of the three Plosky tephra, we assigned them simpler identification codes: PL1 for the lower layer, PL2 for the (most mafic) middle tephra layer, and PL3 to the upper fine-grained tephra (Figs. 4, 13). Thickness measurements of tephra layers as well as direct field tracing of the layers and study of their glass compositions have allowed us to compile isopach maps for PL1 and PL2 (Fig. 11). The number of observations was not enough to constrain reliable isopachs for PL3. PL1 was dispersed NNE from the source (Figs. 4, 11b). Because this tephra is less distinct geochemically, it is difficult to identify it in sections where PL2 tephra is not present and thus where stratigraphy is less clear. The dispersal axis for PL2 goes toward the Kamchatka River mouth (Fig. 11), while the northern margin runs roughly north of Shiveluch volcano. The northern limit of PL2 is constrained by its absence at the Uka site (Fig. 11a; Dirksen et al. 2013), the southern margin lies south of Bezymianny volcano (Fig. 1), and its easternmost limit is constrained by the absence of a visible PL2 layer in a peat profile on Bering Island (Fig. 11a) (Kirianov et al. 1990; Kyle et al. 2011). The most distal terrestrial site where the two larger tephra falls (PL1 and PL2) were described and analyzed is Krutoberegovo village, site JB112 (this study, Fig. 11b; Online Resource 3).

Prior studies have assigned distal tephra layers to Plosky based on stratigraphy and bulk chemical analyses only, and some of those correlations can now be revised or refined. For example, Braitseva et al. (1995) assigned to Plosky (PL2 in this paper) one of the cinder layers sampled at the bottom of the Kliuchi section (sample 1206'-1, Figs. 1, 4). However, our

microprobe data suggest that its glass has a more evolved composition than PL2 (Fig. 13b; Online Resource 3) and may either correlate with some other tephra from the K7-T1 site or may have originated from a flank cinder cone. West of the volcano, we measured and analyzed the early Holocene Plosky package in an archaeological excavation at Ushki-V (Figs. 1, 4) (Dikov 2003; Goebel et al. 2003). Here, all tephra layers are less than 2 cm thick, suggesting that this site lies off the dispersive axes for the two major Plosky tephtras (PL1 and PL2, Fig. 11). The stratigraphic context as well as a relatively evolved composition of glass from these layers, with slightly elevated Cl content (Table 4), allows us to assign these tephtras to eruptions younger than PL2 (e.g., section K7-T1). At Ushki (west of Plosky) as well as in tephra sections located south and southeast of the volcano (Fig. 1), there is no evidence of any other Holocene Plosky tephra packages or layers besides the early Holocene package, which suggests that the above-described eruptive episode comprising PL1 and PL2 large tephtras represents the only significant episode of explosive activity from Plosky volcanic massif during the Holocene.

Western Bering Sea cores

Dark-gray, fine to very fine tephra was sampled in cores SO201-2-77KL (core depth 116–117 cm) and SO201-2-81KL (pilot) (10–13 and 14–17 cm) (Fig. 11a; Dullo et al. 2009). This tephra, coded SR1 during the on-board description, came from semi-liquid sediments enriched in diatoms and carbonate detritus (small, thin-shelled forams and their fragments; coccoliths), which suggests they were deposited during the late glacial—early Holocene warming period (12.4–8.3 cal ka BP according to Gorbarenko 1996; Gorbarenko et al. 2002). In core SO201-2-77KL, strongly bioturbated sediments rich in up to 3-cm-thick tephra lenses are present between 113 and 122 cm. Average thickness of the tephra layer was estimated at 2–3 cm. Microprobe analyses of this tephra show that most of the glass shards in fractions >0.1 and 0.1–0.05 mm match mafic PL2 tephra (Table 4; Figs. 14, 15). Trace element concentrations in these glasses are indistinguishable within 15 rel. % from those in terrestrial PL2 samples and thus confirm the correlation initially based on major element composition of the glasses (Fig. 14). BSE images of these glass shards also support their relation to Plosky tephtras (Fig. 5). In the samples from the pilot core SO201-2-81KL, PL2-like glasses are less abundant but present at both 10–13 and 14–17 cm levels (Online Resource 3), being more abundant in the lower level (Fig. 15). In the finer fractions of the same samples (<0.1 mm in SO201-2-81KL and <0.05 mm in SO201-2-77KL), we found several populations of more silicic glasses (Fig. 15, Online Resource 3) which, with a few exceptions, are different from Plosky glasses.

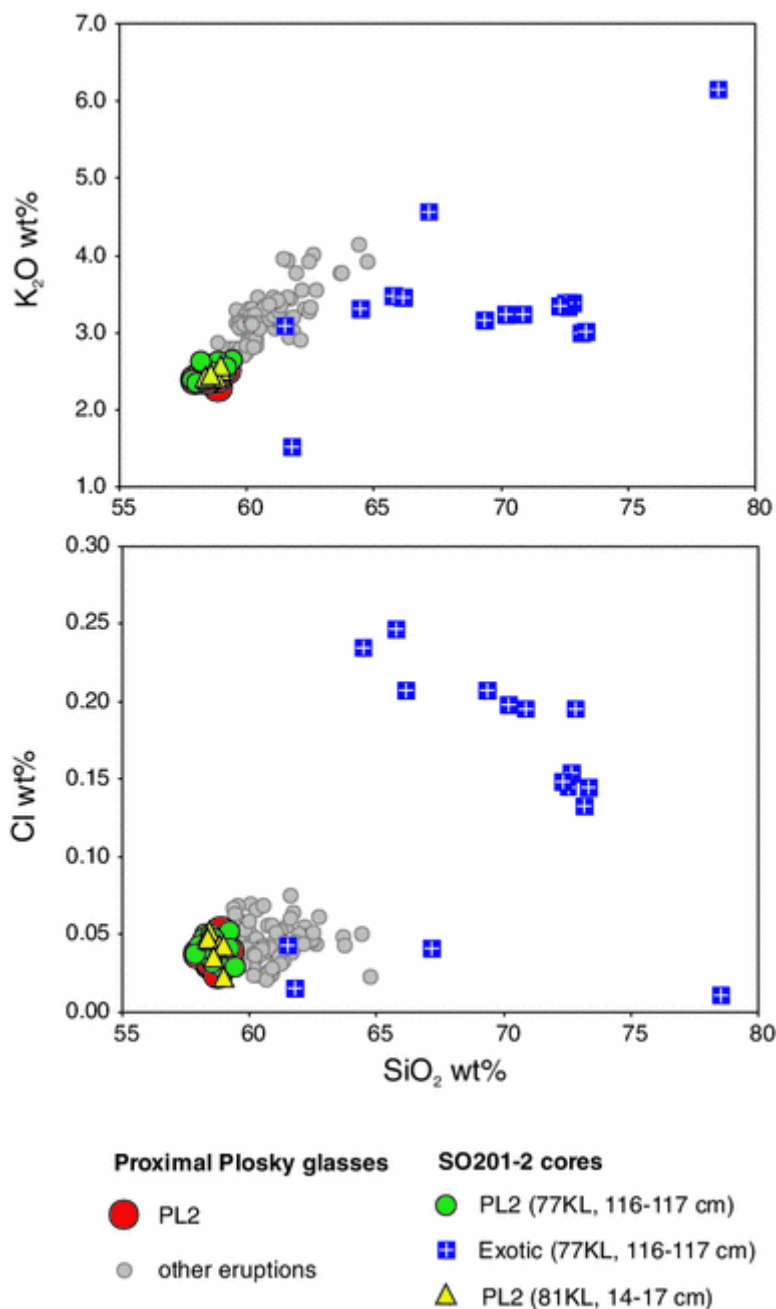


Fig. 15

Graphic plot of glass compositions from the SR1 layer in marine sediment cores from Shirshov Ridge in the Bering Sea (Fig. 11a), compared with proximal Plosky PL2 and other Plosky glasses. Core 81KL is a pilot core

Heavy minerals in the above-described samples were low- and high-Ca pyroxenes, Ti-magnetite, and amphibole, some of which closely resemble minerals in the proximal Plosky samples and thus support the correlation of SR1 with PL2 (Online Resource 2). However, some of the minerals [low-Ti and low-Al low-Ca ($\text{CaO} = 0.9\text{--}1.2$ wt%, $\text{TiO}_2 = 0.14\text{--}0.20$ wt%, $\text{Al}_2\text{O}_3 = 0.4\text{--}1.2$ wt%) and high-Ca ($\text{CaO} = 20.4\text{--}21.4$ wt%, $\text{TiO}_2 = 0.25\text{--}0.40$ wt%, $\text{Al}_2\text{O}_3 = 0.9\text{--}1.8$ wt%) pyroxenes and particularly amphibole] are lacking in Plosky tephras and may be related to the silicic population of glasses from the SR1 layer. The presence of different tephras in the same layers in the marine cores may have resulted from low background accumulation rate, bioturbation, and contamination during the coring. In all these cases, ^{14}C

dates for the Holocene tephra layers obtained in such cores are not likely to be as accurate as those from the detailed terrestrial sections.

In sum, based on tephra stratigraphy as well as on the appearance and composition of glass from terrestrial and marine samples, we correlate K7-T1-12A (PL2) tephra from the Kliuchevskoi slope to coarse tephra found on the slope of Shiveluch and in the Ust'-Kamchatsk area, and farther east to tephra SR1 from Bering Sea cores. Both cores lie on the extended terrestrial axis for this tephra (Fig. 11a), which provides further support for the correlation.

Volumes of PL2 and PL1 tephra and eruption magnitudes

The finding of a 2–3-cm-thick PL2 tephra layer at a distance of >600 km from the source dramatically changes the estimates of its volume calculated from terrestrial deposits only. Legros (2000) proposed a method of estimating the minimum volume of a tephra deposit based on a single isopach. Using his formula $V_{min} = 3.69 TA$ (where T is thickness, and A is area within any isopach) with the terrestrial isopachs 50 and 10 cm, we obtain $V_{min} = 0.34$ and 0.82 km^3 , respectively (Table 5). However, including the data from marine cores (2–3 cm PL2 tephra thickness at site SO201-2-77KL), we obtain minimum volume estimates about an order of magnitude larger— 4.87 – 7.3 km^3 . Calculations based on the method of Bonadonna and Costa (2012) provide an even larger estimate for PL2 volume of 10.4 – 12.3 km^3 for the 2–3 cm layer thickness in the core SO201-2-77KL (Table 5).

Table 5

Volume estimates for Plosky tephra

Tephra	Isopach (cm)	Area (km ²)	V_{min} (km ³), Legros (2000)	Tephra volume (km ³), Bonadonna and Costa (2012)
PL2	50	182.2	0.34	
PL2	10	2,222.7	0.82	
PL2	5	7,118.4	–	
PL2	3	65,927.6	7.3	12.3
PL2	2	65,927.6	4.87	10.4
PL1	2	5,420.1	0.4	–

V_{min} minimum tephra volume

More precise estimates of tephra volume are not possible at this stage as only one distal point

with measured thickness is available. We realize that this thickness could differ from the original one because of bioturbation or other processes. At the same time, we note that although PL2 tephra is not expressed as a distinct layer in the neighboring core SO201-2-81KL, it is mixed into the sediments in a thick interval between 10 and 17 cm with a peak at 14–17 cm, so its original thickness could be similar to that in core SO201-2-77KL. Both cores lie at the extension of the terrestrial tephra fall axis (Fig. 11a). In addition, the dominantly large grain size (>0.1 mm) of PL2 (SR1) ash in the inspected cores suggests that the real area of dispersal of finer ash could be far larger, so even the larger calculated values of PL2 volume may be quite conservative. These values allow us to estimate the magnitude of PL2 eruption at 6.0–6.1 (based on calculations proposed by Pyle (1995, 2000); at a measured cinder density of 1.1 g/cm^3 and erupted mass of 11.44–13.53 Gt). Minimum volume of the lava flows following the PL2 tephra eruption is estimated at $\sim 2 \text{ km}^3$ assuming an average thickness of 10 m (Fig. 1).

The older PL1 tephra yields smaller bulk volume (0.4 km^3) and (Pyle method) eruption magnitude (4.6) compared to PL2. These estimates, however, are based on terrestrial measurements only and may significantly increase if distal PL1 tephra were found offshore. Other Plosky tephtras including PL3 are less thick and extensive, hence smaller in volume to PL1 and PL2 and likely not exceeding 0.1 km^3 .

Age estimates for Plosky tephtras

Radiocarbon dating of organic matter associated with tephra material offers the best age estimates for Holocene tephra in Kamchatka. For PL1 and PL2 Plosky tephtras, we base our age estimates on ^{14}C measurements obtained at distal terrestrial site JB112 (Figs. 4, 11b) because no datable materials are available in proximal sections. The age of PL1 was obtained on a pollen aliquot from inside the tephra (at 683–682 cm depth). The obtained date of $10,080 \pm 40 \text{ BP}$ (Beta-320735) provides the most probable 2-sigma calendar interval for this eruption of 11,397–11,825 cal BP with the median probability at $\sim 11,650$ cal BP. The sample for dating PL2 is a combination of pollen and leaf fragments from *Isoetes* spp. collected from the lower part of the PL2 cinder layer at a depth of 669.5–669 cm. These leaves and pollen were buried by 6-cm-thick PL2 tephra; hence, the dated material should provide the best age estimate for the tephra. The obtained date of $9,040 \pm 50 \text{ BP}$ (Beta-305867) provides the most probable 2-sigma calendar interval for the PL2 eruption of 10,146–10,287 cal BP with the median probability at $\sim 10,200$ cal BP (Stuiver and Reimer 1986; Stuiver and Reimer 1993; Reimer et al. 2009). This date fits well in the stratigraphic succession on Shiveluch and elsewhere (Fig. 4; Pevzner et al. 2012). The uppermost marker tephra in Plosky package (PL3 at Figs. 4, 12) is likely only ~ 120 year younger than PL2 based on the average accumulation rate for the K7-T1 sequence of $\sim 1 \text{ mm/year}$ (Portnyagin and Ponomareva 2012) and a thickness of sandy loam between these Plosky layers of 12 cm.

Braitseva et al. (1995) reported two dates for the main Plosky tephra (PL2) obtained from bulk

paleosol samples: $8,610 \pm 60$ ^{14}C years from below the tephra in Kliuchi town (site 1206, sample 1206'-1) and $8,620 \pm 100$ ^{14}C years from above the coarse tephra in Kamaki, site 58 (Figs. 1, 4, 11). However, as discussed above, Kliuchi sample 1206'-1, collected above the dated paleosol, does not match the PL2 tephra geochemically (Fig. 13b; Online Resource 3) and may represent some other tephra from the Plosky package. Therefore, the date of $8,610 \pm 60$ ^{14}C years is not valid for (below) PL2. The dates of $8,620 \pm 100$ years in site 58 (Braitseva et al. 1995) and $8,670 \pm 80$ ^{14}C years from a proximal section at Shiveluch slope (Ponomareva et al. 2007b) were obtained above PL2 tephra and do not contradict the newly obtained date.

Discussion

PL2 eruption

The PL2 eruption produced 10–12 km³ of tephra fall deposits dispersed over an area of >70,000 km². Virtually, no very fine ash (<0.05 mm) has been reported either in proximal or distal PL2 tephra. A low proportion of very fine ash is typical for mafic tephra and may be explained in part by lack of pyroclastic flows in these eruptions and thus low rate of secondary comminution of pyroclasts (Rose and Durant 2009). Indeed, the PL2 eruption did not produce ignimbrites, so co-ignimbrite ash did not contribute to the distal fall deposits. Far larger dispersal area and volume of PL2 tephra than expected from its terrestrial deposits (Table 5) might prompt that even for relatively mafic tephra with only a small, if any, amount of very fine ash, a large proportion of the deposit can be missed if the volume calculations rely only on proximal deposits.

The PL2 eruption appears to be one of the largest Holocene explosive events known in Kamchatka, exceeding in tephra volume the largest reported eruptions from highly explosive andesitic volcanoes Shiveluch (SH₂, 2.5 km³) and Avachinsky (IAv₂, ≥ 8 –10 km³) and approaching volumes of caldera-forming eruptions at Ksudach (KS₂ + KS₃, 9–11 km³) and Karymsky (13–16 km³) (Braitseva et al. 1997a, 1998; Ponomareva et al. 2007b). This reevaluation of eruptive volume further suggests that the smaller, 4 km-wide Holocene summit caldera at Ushkovsky volcano likely formed as a result of the catastrophic PL2 eruption rather than as a result of lava effusion as previously thought (Melekestsev et al. 1974; Braitseva et al. 1995).

Early Holocene time (12–10 cal ka BP) in Kamchatka was not previously regarded as a period of large explosive eruptions but rather as a time of dominantly mafic eruptions with only moderate explosive activity (Braitseva et al. 1995, 1997b; Melekestsev et al. 1974; Ponomareva et al. 2007a). Our data, however, suggest that the onset of the described explosive activity from Plosky is close in time to recently dated onset of neighboring Shiveluch vigorous explosive activity (Pevzner et al. 2012). Our ongoing detailed studies of early Holocene tephra in the area should

allow us to reconsider explosive activity of this period and also permit better understanding of the temporal patterns in eruptive activity over the entire volcanic arc.

Plosky eruptive activity in early Holocene time

The compact stratigraphic position of Plosky tephra in all studied sections suggests a single early Holocene episode of activity from the volcano. It started about 11,650 cal BP with a $M \sim 4.6$ explosive eruption (PL1) and probably formation of some cinder cones in the northeastern part of the rift zone, followed by $\sim 1,000$ years of weak activity recorded by several thin tephra layers enclosed in sandy loam (Fig. 4). About 10,200 cal BP, there was a violent explosive eruption (PL2) with (Pyle method) $M_{6.0-6.1}$, followed by a few weak eruptions including PL3. All explosive eruptions were magmatic with no obvious phreatic component. Explosive activity was followed by profuse low-viscosity lava flows with a total volume of $>2 \text{ km}^3$. The whole eruptive episode lasted for $\sim 1,500$ years and is the only known Holocene activity from Plosky volcanic massif.

A rift-like structure, superimposed on the Plosky massif (Fig. 1), consists of NNE-trending rifts with a right-lateral strike-slip component probably accommodating high extension rates and high magma supply in this part of the Central Kamchatka depression, related to oceanward stretching of the arc crust (Kozhurin 2009). The structure resembles rifts on Mauna Loa, Mauna Kea, Etna, and other shield volcanoes albeit on a smaller scale. In Kamchatka, the closest analogues are as follows: a zone of cinder cones, which crosses Plosky Tolbachik volcano (Fig. 1); the fissure feeding the most recent lava flows from Gorely volcano (Selyangin and Ponomareva 1999); and probably a rift structure which crosses Krasheninnikov volcano and caldera (Ponomareva 1990). All these volcanoes host summit calderas or unusually large nested craters. Another common feature of all these volcanoes is a tholeiitic evolution trend in magmas erupted along the rift zones (Volynets 1994).

As we showed above, high-K and medium-K rock series of Plosky volcanic massif originated from different parental magmas. The early Holocene activity from Plosky which produced high-K rocks was related to a superimposed rift structure where magma partly exploited pathways that earlier had fed medium-K chamber of Ushkovsky stratovolcano. In the same way, high-K basalts from Plosky Tolbachik Holocene eruptions were produced by a regional rift zone rather than by the stratovolcano itself (Ermakov and Vazheevskaya 1973; Braitseva et al. 1983). At Tolbachik (Fig. 1), the same pathways in the rift zone were also used by a very different type of magma—medium-K high-Mg basalt—which first appeared 1,600 cal BP and later erupted repetitively along with the dominating high-K subalkaline basalts (Braitseva et al. 1983). Magma erupted during the early Holocene Plosky activity is not the same as that of Tolbachik high-K basalts, but they both are probably related to basalts–basaltic andesites of the shield volcano preceding Ushkovsky and Krestovsky stratovolcanoes, and plateau lavas comprising the Kliuchevskoi group basement (Churikova et al. 2001; Portnyagin et al. 2007). To date, all these

high-K basalts–basaltic andesites are the oldest and the most voluminous magmatic component for the Kliuchevskoi group rocks, which has been persisting throughout its activity starting from at least mid-Pleistocene time (Melekestsev et al. 1974; Calkins 2004).

Activity of the Plosky rift zone last surged in the early Holocene and then waned soon after 10,200 cal BP, close to the time when the Tolbachik zone started to form (Braitseva et al. 1983), that is, the Plosky rift was replaced by the new Tolbachik one. This was a major reorganization of volcanic structures in the western part of the Kliuchevskoi volcanic group, probably related to some changes in the parameters of oceanward stretching of the crust driven by dynamics of the dangling Pacific slab (Park et al. 2002; Kozhurin 2009).

Marker tephra layers from Plosky

Plosky tephra (PL2 especially) is exceptional because andesitic tephra is frequently considered to be less important for regional tephrochronology compared to more silicic ones. In general, andesitic tephra has relatively small tephra volumes and dispersal areas and is not well preserved (Cronin et al. 1996; Platz et al. 2007). They also are considered difficult for geochemical fingerprinting because of large heterogeneity in glass (which reflects mixing of different magmas prior to the eruption) (Shane et al. 2005; Donoghue et al. 2006) and because of high crystallinity that hampers reliable glass analyses (Platz et al. 2007). On the contrary, PL2 basaltic andesite–andesitic tephra has large volume and dispersal area, is dominantly vitric, and is characterized by quite homogeneous glass composition. Whereas cindery tephra are rarely used as markers because they look alike in the field and cannot be easily traced from one section to another, distinctive petrographic features and geochemical composition of PL cindery tephra permit their identification and thus use as markers.

Distinctive petrographic and geochemical features of the PL2 tephra useful for its identification and correlation include the following: (1) predominantly vitric sponge-shaped fragments with very rare phenocrysts and microlites of plagioclase, olivine, and pyroxenes; (2) medium- to high-K basaltic andesitic bulk composition; (3) high-K, high-Al, and high-P trachyandesitic glass composition ($\text{SiO}_2 = 57.5\text{--}59.5$ wt%, $\text{K}_2\text{O} = 2.3\text{--}2.7$ wt%, $\text{Al}_2\text{O}_3 = 15.8\text{--}16.5$ wt%, $\text{P}_2\text{O}_5 = 0.5\text{--}0.7$ wt%); and (4) typical subduction-related pattern of incompatible elements, high concentrations of all REE ($>10\times$ mantle values), moderate enrichment in LREE ($\text{La/Yb} \sim 5.3$), and non-fractionated pattern of Cs, Rb, Ba, and U (i.e., mantle-normalized Ba/Rb, Ba/U, etc., are close to 1).

PL1 tephra is compositionally similar to some younger Plosky tephra produced by weaker eruptions (including PL3), so it has a less distinct geochemical signature than PL2. However, it is a good marker for Shiveluch and Kliuchevskoi slopes as well as for the area east of Shiveluch (Fig. 11), where both PL2 and PL1 are present (Fig. 4 and other sections). Compared to PL2, PL1 glass has a more silicic composition ($\text{SiO}_2 = 59.6\text{--}61.5$ wt%) and higher K_2O content (2.9–3.4 wt%). PL1 is an important marker for the late glacial–Holocene transition and is thus

far the oldest dated and geochemically characterized marker tephra layer in Kamchatka. PL3 tephra is a good marker in the sections at the south slope of Shiveluch volcano where it has distinct stratigraphic position (Fig. 12) and is finer grained than PL1 or PL2 tephras.

On land, Plosky tephra layers are good markers for dating and synchronizing records of early Holocene volcanism (eruptive activity; petrological, and geochemical variations in erupted products), tectonic (faulting events), environmental changes (pollen, macrofossils), and human occupation currently emerging for this area (e.g., Ponomareva et al. 2007b; Dirksen et al. 2013; Pinegina et al. 2012; Hulse et al. 2011). The whole Plosky tephra package may serve as a composite marker in some studies. For example, in Ushki archaeological site, the whole Plosky package falls between levels 5 and 6 of human occupation (Dikov 2003) (Fig. 4). Level 6 was dated to ~13,200–11,200 cal BP (Goebel et al. 2003) and level 5 to $\sim 8,790 \pm 150$ ^{14}C year BP (9,536–10,204 cal BP) by Dikov (2003) and $\sim 7,640 \pm 80$ ^{14}C year BP (8,317–8,596 cal BP) by Goebel et al. (2003). Based on our stratigraphy, we would favor the latter age estimate for the level 5 because it lies distinctly higher in the section than the Plosky package and thus should be younger than 10,000 cal BP.

Terrestrial–marine correlation of individual tephra layers provides an excellent tool for direct comparisons between terrestrial and marine paleoclimate records (e.g., Davies et al. 2008; Lowe 2011). Major Plosky tephra PL2 was found in Bering Sea cores at a distance of >600 km from the source. This is the second Holocene Kamchatka tephra with a known source identified in marine cores; the other is the KO tephra associated with the Kurile Lake caldera (Gorbarenko et al. 2002). PL2 is the only Holocene tephra thus far identified in marine cores on the east side of the peninsula. The PL2 tephra layer serves as an isochrone for sediment sequences over an area of >70,000 km² and is a tie point for comparing and dating terrestrial and marine paleoclimate records near the early Holocene Pre-Boreal–Boreal transition. A high-quality new ^{14}C date from a terrestrial excavation restricts its most probable age to a short interval of 10,146–10,287 cal BP and provides a great age constraint for early Holocene marine deposits in the southwestern Bering Sea.

Reservoir age for the western Bering Sea in early Holocene time

Our finding of PL2 tephra both in the terrestrial and marine sediments allows us to estimate for the first time a reservoir age for the western Bering Sea. Carbonate samples from the ocean surface have an apparent radiocarbon age ~400 years older on average than contemporaneous terrestrial samples (Stuiver and Braziunas 1993). This offset or *reservoir age* is known as R(t) and is built into the marine calibration curve (currently Marine09). The regional value of R(t) is time dependent, while ΔR , *the deviation from the average ocean surface age*, is constant to a first approximation (Stuiver and Braziunas 1993). To calibrate marine radiocarbon ages, the regional deviation needs to be estimated and the ages corrected or calibrated with the marine calibration curve. It is also possible to calibrate by subtracting R(t) from the sample radiocarbon

age and use the atmospheric calibration curve (currently IntCal09), but because the ocean attenuates the atmospheric signal, this is not the generally accepted procedure. The virtually instantaneous deposition of tephra over onshore and offshore areas permits comparison of stratigraphically related on-land and marine ^{14}C dates and calculations of reservoir age ($R(t)$) and of deviation from the average ocean surface age (ΔR) (e.g., Ascough et al. 2004; Eiriksson et al. 2004; Thornalley et al. 2011). In locations where both marine and terrestrial samples are deposited, $R(t)$ can be calculated from the difference in radiocarbon age between the marine and terrestrial sample.

Estimates of the reservoir age for the western Bering Sea are lacking, so, in order to calibrate marine radiocarbon ages, researchers have to use $\Delta R = 698 \pm 50$ ^{14}C years obtained ~2,000 km southwest, at Sakhalin Island in the Okhotsk Sea (Kuzmin et al. 2007), or a value from two known age shells of *Mytilus edulis* from ~1,550 km northeast at Port Clarence, Alaska, which yield a mean ΔR and standard deviation of 497 ± 83 ^{14}C years (McNeely et al. 2006).

We presume that the deposition of PL2 tephra on land and on the seafloor represented in core SO201-2-77KL was virtually instantaneous despite several caveats. Stratigraphic position of a tephra layer in marine sediments may be distorted due to various factors. Tephra particles may sink through soft organic-rich sediments and occur lower in a core than its original stratigraphic position as described for the lake deposits (e.g., Beierle and Bond 2002). Tephra also can be deposited from icebergs with some delay and thus occur higher in the section (Brendryen et al. 2010). In case of PL2 tephra in the core SO201-2-77KL, however, none of these complications seem likely because the PL2 ash (though bioturbated) forms quite a distinct layer (Dullo et al. 2009), the axis of the distal ash coincides with that for the terrestrial PL2 tephra (Fig 11a), and the glaciers did not reach the coast in early Holocene, so iceberg formation at this time is unlikely (Melekestsev et al. 1974).

Dates for PL2 tephra obtained on both terrestrial and marine materials allow us to make a tentative estimate reservoir ages for the western Bering Sea in the early Holocene. Max et al. (2012) published an AMS ^{14}C age of $10,450 \pm 40$ BP (OS-85658) on the planktonic foraminifera sampled in the core SO201-2-77KL at a depth of 115–116 cm immediately above the PL2 tephra. Using the terrestrial radiocarbon date of $9,040 \pm 50$ BP discussed above and this marine date, we calculate $R(t) = 1,410 \pm 64$ and $\Delta R = 1,064 \pm 55$ for this time period using the Marine09 and IntCal09 curves following the method of Stuiver and Braziunas (1993). Because the dated foraminifera had to have been deposited slightly later than the PL2 tephra, these numbers provide just a minimum estimate. The calculated $R(t)$ and ΔR values for the western Bering Sea are much larger than expected from the modern estimates detailed above; however, they are close to estimates for the last glacial period $R(t)$ of ~2,000 ^{14}C years from the southwest Pacific (Sikes et al. 2000). We treat our calculated values as tentative because they are based on one pair of samples only, and the relative position of PL2 tephra and the dated foraminifera could have been influenced by bioturbation of the sediments (or mixing during coring).

Conclusions: lessons from this study

Obviously, the mapping of tephra distribution from eruptions in island arcs and from other volcanoes where winds carry eruptive products offshore is a challenge without offshore sampling. Moreover, because of the “soupy” nature of Holocene sediments in many marine cores, identification of tephra and assessing of its original stratigraphic position require careful sampling and analysis. In the case of the early Holocene Plosky PL2 tephra studied herein, the discovery of tephra offshore was fortuitous because marine cores were taken (for other reasons) along the axis of ash dispersal, which was in fact not well known when the cores were taken. The discovery of the PL2 tephra offshore dramatically increases its volume calculations, and this must be the case for many other tephra; we urge those taking marine cores to pay particular attention to the possibility of tephra presence—even if not well preserved in a layer, tephra presence can be an important component to mapping the tephra and calculating eruptive volume, which in turn affects both scientific and hazard evaluations of volcanic activity. Moreover, the correlation of a <50 ka old tephra in both terrestrial and marine settings provides the important possibility of paired ^{14}C dates and thus for calculations of local marine reservoir ages.

Our tephrochronological studies, including geochemical fingerprinting, in the highly productive Kliuchevskoi volcanic group have allowed us to document an early Holocene eruptive episode of medium- to high-K basaltic andesites—andesites from Ushkovsky volcano (Plosky volcanic massif), consisting of a suite of explosive eruptions followed by profuse lava flows. This eruptive episode was followed by a major reorganization of volcanic structures in the western part of the Kliuchevskoi volcanic group, probably related to some changes in the parameters of oceanward stretching of the crust. The more mafic composition of the PL2 tephra and yet its high volume and broad distribution is of particular interest. The PL2 eruption produced 10–12 km³ of tephra fall deposits dispersed over an area of >70,000 km². Virtually, no very fine ash (<0.05 mm) has been reported in either proximal or distal PL2 tephra. A low proportion of very fine ash is typical for mafic tephra and may be explained in part by lack of pyroclastic comminution; indeed, the PL2 eruption did not produce ignimbrites. The lesson from this case is that even for relatively mafic tephra with little very fine ash, the total eruptive volume can be significantly underestimated if relying only on proximal deposits.

Our findings suggest that PL2 was one of the larger Holocene explosive eruptions in Kamchatka, yielding a tephra volume of 10–12 km³ and magnitude of ~6. PL2 tephra was ^{14}C -dated at ~10,200 cal BP, making it a valuable marker for the study of early Holocene climate fluctuations, for example, the Pre-Boreal–Boreal transition. This correlation permits direct links between terrestrial and marine paleoenvironmental records. We have also documented a second early Holocene (late Glacial), voluminous tephra from the Plosky massif (PL1) in terrestrial sections and dated it at ~11,650 cal BP. The measured age of PL1 and possibility to identify it geochemically, particularly when it occurs together with PL2, makes it an important local marker

for Younger Dryas—early Holocene transition. PL1 is thus far the oldest dated and geochemically characterized marker tephra layer in Kamchatka. One more tephra from Plosky, coded PL3, is ~120 years younger than PL2. Compositionally, it is close to PL1 tephra and can be used as a marker northeast of the source at a distance of ~110 km, in the sections where PL1 and PL2 are also present.

Acknowledgments

The major part of this research was supported by the KALMAR project funded by the Bundesministerium für Bildung und Forschung (BMBF) (Germany). Plosky tephra in site JB112 (Ust'-Kamchatsk area) was studied and dated thanks to US National Science Foundation project #0915131 to Ezra Zubrow. Many years of earlier field research, which, along with their other goals, have allowed us to measure and sample Plosky tephra in various distant places, have been funded by the grants from the National Geographic Society and the Russian Foundation for Basic Research. Studies of submarine tephra were partly funded by grants #11-05-00506 and 13-05-00346 from the Russian Foundation for Basic Research. The authors thank Maria Pevzner for the samples from the Shiveluch southeastern slopes, Mario Thöner (GEOMAR) and Nikita Mironov (GEOKHI) for their help with the microprobe analysis and sample preparation, and Dmitry Melnikov and Egor Zelenin for their help with graphics and tephra volume calculations. Thorough reviews of Sabine Wulf and an anonymous reviewer are very much appreciated.

Electronic supplementary material

Below is the link to the electronic supplementary material.

Supplementary material 1 (PDF 39 kb)

Supplementary material 2 (XLS 91 kb)

Supplementary material 3 (XLS 262 kb)

References

- Arculus RJ (2003) Use and abuse of the terms calcalkaline and calcalkalic. *J Petrol* 44:929–935
CrossRef
- Ascough PL, Cook GT, Dugmore AJ, Barber J, Higney E, Scott EM (2004) Holocene variations in the Scottish marine radiocarbon reservoir effect. *Radiocarbon* 46(2):611–620

Auer S, Bindeman I, Wallace P, Ponomareva V, Portnyagin M (2009) The origin of hydrous, high- $\delta^{18}\text{O}$ voluminous volcanism: diverse oxygen isotope values and high magmatic water contents within the volcanic record of Klyuchevskoy volcano, Kamchatka, Russia. *Contrib Miner Petrol* 157(2):209–230

[CrossRef](#)

Bazanova LI, Pevzner MM (2001) Khangar: one more active volcano in Kamchatka. *Trans Russ Acad Sci Earth Sci* 377A:307–310

Beierle B, Bond J (2002) Density-induced settling of tephra through organic lake sediments. *J Paleolimnol* 28:433–440

[CrossRef](#)

Bonadonna C, Costa A (2012) Estimating the volume of tephra deposits: a new simple strategy. *Geology* 40:415–418

[CrossRef](#)

Bourgeois J, Pinegina TK, Ponomareva VV, Zaretskaia NE (2006) Holocene tsunamis in the southwestern Bering Sea, Russian Far East and their tectonic implications. *Geol Soc Am Bull* 11(3/4):449–463. doi:10.1130/B25726.1

[CrossRef](#)

Braitseva OA, Melekestsev IV, Ponomareva VV (1983) Age divisions of the Holocene volcanic formations of the Tolbachik Valley. In: Fedotov SA, Markhinin YK (eds) *The great Tolbachik fissure eruption: geological and geophysical data 1975–1976*. Cambridge Earth Sci. Series, vol 341, pp 83–95

Braitseva OA, Sulerzhitsky LD, Litasova SN, Grebzdzy EI (1988) Radiocarbon dating of soils and pyroclastic deposits in Kliuchevskoi group of volcanoes. *Volcanol Seismol* 6:317–325

Braitseva OA, Melekestsev IV, Ponomareva VV, Sulerzhitsky LD (1995) The ages of calderas, large explosive craters and active volcanoes in the Kuril-Kamchatka region, Russia. *Bull Volcanol* 57(6):383–402

Braitseva OA, Sulerzhitsky LD, Ponomareva VV, Melekestsev IV (1997a) Geochronology of the greatest Holocene explosive eruptions in Kamchatka and their imprint on the Greenland glacier shield. *Trans Russ Acad Sci Earth Sci* 352(1):138–140

Braitseva OA, Ponomareva VV, Sulerzhitsky LD, Melekestsev IV, Bailey J (1997b) Holocene key-marker tephra layers in Kamchatka, Russia. *Quat Res* 47:125–139

[CrossRef](#)

Braitseva OA, Bazanova LI, Melekestsev IV, Sulerzhitsky LD (1998) Largest Holocene

eruptions of Avachinsky volcano, Kamchatka. *Volcanol Seismol* 20:1–27

Brendryen J, Haflidason H, Sejrup HP (2010) Norwegian Sea tephrostratigraphy of marine isotope stages 4 and 5: prospects and problems for tephrochronology in the North Atlantic region. *Quat Sci Rev* 29(7–8):847–864

CrossRef

Calkins J (2004) $^{40}\text{Ar}/^{39}\text{Ar}$ geochronology of Khapitsa Plateau and Studyonaya River basalts and basaltic andesites in Central Kamchatka Depression, Kamchatka, Russia. Abstracts of the IV Int Workshop on Subduction Processes emphasizing the Japan-Kurile-Kamchatka-Aleutian Arcs (JKASP) <http://www.kscnet.ru/ivs/conferences/kasp/tez/contents.htm>

Churikova T, Dorendorf F, Wörner G (2001) Sources and fluids in the mantle wedge below Kamchatka, evidence from across-arc geochemical variation. *J Petrol* 42(8):1567–1593

CrossRef

Cronin SJ, Neall VE, Stewart RB, Palmer AS (1996) A multiple-parameter approach to andesitic tephra correlation, Ruapehu volcano, New Zealand. *J Volcanol Geotherm Res* 72:199–215

CrossRef

Davies SM, Wastegård S, Rasmussen TL, Johnsen SJ, Steffensen JP, Andersen KK, Svensson A (2008) Identification of the Fugloyarbanki tephra in the NGRIP ice-core: a key tie-point for marine and ice-core sequences during the last glacial period. *J Quat Sci* 23:409–414

CrossRef

Dikov NN (2003) *Archaeological Sites of Kamchatka, Chukotka, and the Upper Kolyma*. Anchorage, Alaska: U.S. Department of the Interior, National Park Service, Shared Beringian Heritage Program

Dirksen V, Dirksen O, Diekmann B (2013) Holocene vegetation dynamics in Kamchatka, Russian Far East. *Rev Palaeobot Palynol* 190:48–65

Donoghue SL, Vallance J, Smith IEM, Stewart RB (2006) Using geochemistry as a tool for correlating proximal andesitic tephra: case studies from Mt Rainier (USA) and Mt Ruapehu (New Zealand). *J Quat Sci* 22(4):395–410

CrossRef

Duggen S, Portnyagin M, Baker J, Ulfbeck D, Hoernle K, Garbe-Schönberg D, Grassineau N (2007) Drastic shift in lava geochemistry in the volcanic-front to rear-arc region of the Southern Kamchatkan subduction zone: evidence for the transition from slab surface dehydration to sediment melting. *Geochim Cosmochim Acta* 71:452–480

CrossRef

Dullo C, Baranov B, Bogaard Cvd (2009) RV Sonne Fahrtbericht/Cruise Report SO201-2: KALMAR (Kurile-Kamchatka and Aleutian Marginal Sea-Island Systems): Geodynamic and Climate Interaction in Space and Time. IFM-GEOMAR Report 35: <http://www.ifm-geomar.de/index.php?id=publikationen>

Eiriksson J, Larsen G, Knudsen KL, Heinemeier J, Simonarson LA (2004) Marine reservoir age variability and water mass distribution in the Iceland Sea. *Quat Sci Rev* 23(20–22):2247–2268
CrossRef

Ermakov VA, Vazheevskaya AA (1973) Ostry and Plosky Tolbachik volcanoes. *Bull Volcanol Stn* 49:36–43 (In Russian)

Flerov GB, Ovsyannikov AA (1991) Ushkovsky volcano. In: Fedotov SA, Masurenkov YuP (eds) *Active volcanoes of Kamchatka*, vol 1. Nauka, Moscow, pp 84–92

GeoReM (2011) Geological and environmental reference materials. <http://georem.mpch-mainz.gwdg.de/>. Accessed 2011

Gill JB (1981) *Orogenic andesites and plate tectonics*. Springer, Berlin, p 390
CrossRef

Goebel T, Waters MR, Dikova M (2003) The archaeology of Ushki Lake, Kamchatka, and the Pleistocene peopling of the Americas. *Science* 301:501–505
CrossRef

Gorbarenko SA (1996) Stable isotope and lithological evidence of late-glacial and Holocene oceanography of the Northeastern Pacific and its marginal seas. *Quat Res* 46:230–250
CrossRef

Gorbarenko SA, Nuernberg D, Derkachev AN, Astachov AS, Southon JR, Kaiser A (2002) Magnetostratigraphy and tephrochronology of the Upper Quaternary sediments in the Okhotsk Sea: implication of terrigenous, volcanogenic and biogenic matter supply. *Marine Geol* 183:107–129
CrossRef

Gorbatov A, Kostoglodov V, Suarez G, Gordeev EI (1997) Seismicity and structure of the Kamchatka subduction zone. *J Geophys Res B* 102(8):17,883–17898

Herz O (1897) *Reise von Jakutsk nach Kamtschatka im Jahre 1890*. *Memoires sur les Lepidopteres* 9:239–299

Hulse EL, Keeler DM, Zubrow EBW, Korosec GJ, Ponkratova IY, Curtis C (2011) A preliminary report on archaeological fieldwork in the Kamchatka Region of Russia. *Sibirica* 1:48–74
CrossRef

Jull M, McKenzie D (1996) The effect of deglaciation on mantle melting beneath Iceland. *J Geophys Res* 101(B10):21815–21828. doi:10.21029/21896JB01308

CrossRef

Kirianov VYu, Egorova IA, Litasova SN (1990) Volcanic ash on Bering Island (Commander Islands) and Kamchatkan Holocene eruptions. *Volcanol Seismol* 8:850–868

Kozhurin A (2009) A dangling slab and arc-normal extension: the case of Kamchatka, Russia. *Eos Trans AGU*, 90(52), Fall Meet Suppl, Abstract T41C-2034

Kozhurin A, Acocella V, Kyle PR, Lagmay FM, Melekestsev IV, Ponomareva V, Rust D, Tibaldi A, Tunesi A, Corazzato C, Rovida A, Sakharov A, Tengonciang A, Uy H (2006) Trenching active faults in Kamchatka, Russia: paleoseismological and tectonic implications.

Tectonophysics 417:285–304

CrossRef

Krashennnikov SP (2008) Petrological characteristics of the early Holocene pyroclastic rocks from the northeastern slope of Kliuchevskoi volcano. Bachelor's Diploma Thesis. Moscow State University. Geology Department, p 65. (In Russian)

Kuehn SC, Froese DG, Shane PAR (2011) The INTAV intercomparison of electron-beam microanalysis of glass by tephrochronology laboratories, results and recommendations. *Quat Int.* doi:10.1016/j.quaint.2011.08.022

Kuzmin YV, Burr GS, Gorbunov SV, Rakov VA, Razjigaeva NG (2007) A tale of two seas: reservoir age correction values (R, DR) for the Sakhalin Island (Sea of Japan and Okhotsk Sea). *Nucl Instrum Methods Phys Res B* 259:460–462

CrossRef

Kyle PhR, Ponomareva VV, Rourke Schlupe R (2011) Geochemical characterization of marker tephra layers from major Holocene eruptions in Kamchatka, Russia. *Int Geol Rev* 53(9):1059–1097

CrossRef

Le Bas MJ, Le Maitre RW, Streckeisen A, Zanettin B (1986) A chemical classification of volcanic rocks based on the total alkali-silica diagram. *J Petrol* 27:745–750

CrossRef

Legros F (2000) Minimum volume of a tephra fallout deposit estimated from a single isopach. *J Volcanol Geotherm Res* 96:25–32

CrossRef

Lowe DJ (2011) Tephrochronology and its application: a review. *Quat Geochronol* 6:107–153

CrossRef

Max L, Riethdorf J-R, Tiedemann R, Smirnova M, Lembke-Jene L, Fahl K, Nürnberg D, Matul A, Mollenhauer G (2012) Sea surface temperature variability and sea-ice extent in the subarctic northwest Pacific during the past 15,000 years. *Paleoceanography* 27:PA3213. doi:10.1029/2012PA002292

CrossRef

McDonough WF, Sun S-S (1995) The composition of the Earth. *Chem Geol* 120:223–253

CrossRef

McNeely R, Dyke AS, Southon JR (2006) Canadian marine reservoir ages, preliminary data assessment. *Open File Rep Geol Surv Can* 5049:3

Melekestsev IV (2005) Mt. Sredny (Kliuchevskoi volcanic group, Kamchatka) is a gigantic allochthon rather than a separate volcano. *Volcanol Seismol* 3:9–14 (In Russian)

Melekestsev IV, Braitseva OA, Erlich EN, Kozhemyaka NN (1974) Volcanic mountains and plains. In: Luchitsky IV (ed) *Kamchatka, Kurile and Commander Islands*. Nauka, Moscow, pp 162–234 (in Russian)

Melekestsev IV, Khrenov AP, Kozhemyaka NN (1991) Tectonic position and general description of volcanoes of Northern group and Sredinny Range. In: Fedotov SA, Masurenkov YuP (eds) *Active volcanoes of Kamchatka, vol 1*. Nauka, Moscow, pp 79–81

Miyashiro A (1974) Volcanic rock series in island arcs and active continental margins. *Am J Sci* 274(4):321–355

CrossRef

Ovsyannikov AA, Khrenov AP, Muraviev YaD (1985) Present fumarolic activity on Dalny Plosky volcano. *Volcanol Seismol* 5:80–97 (In Russian)

Park J, Levin V, Brandon M, Lees J, Peyton V, Gordeev E, Ozerov A (2002) A dangling slab, amplified arc volcanism, mantle flow and seismic anisotropy in the Kamchatka plate corner. In: Stein S and Freymueller JT (Eds) *Plate boundary zones: AGU Geodynamics Series, vol 30*, pp 295–324

Pevzner MM, Tolstykh ML, Babansky AD, Kononkova NN (2012) Reorganization of the magmatic system of the Shiveluch volcanic massif as a consequence of the large-scale collapses of its edifice in late Pleistocene-early Holocene times. *Doklady Earth Sciences* (in press)

Piip BI (1956) Kliuchevskaya Sopka and its eruptions in 1944–1945 and the Past. *Trans Volc Lab AN SSSR, Issue 11* (in Russian)

- Pinegina TK, Bourgeois J (2001) Historical and paleo-tsunami deposits on Kamchatka, Russia: long-term chronologies and long-distance correlations. *Nat Hazards Earth Syst Sci* 1:177–185
CrossRef
- Pinegina TK, Kozhurin AI, Ponomareva VV (2012) Seismic and tsunami hazard for Ust'-Kamchatsk village (Kamchatka) based on paleoseismological data. *Vestnik KRAUNZ* 1:138–159 (In Russian)
- Platz T, Cronin SJ, Smith IEM, Turner MB, Stewart RB (2007) Improving the reliability of microprobe-based analyses of andesitic glasses for tephra correlation. *The Holocene* 17(5):573–583
CrossRef
- Ponomareva VV (1990) The history of Krasheninnikov volcano and the dynamics of its activity. *Volcanol Seismol* 9:714–741
- Ponomareva VV, Churikova TG, Melekestsev IV, Braitseva OA, Pevzner MM, Sulerzhitsky LD (2007a) Late Pleistocene-Holocene Volcanism on the Kamchatka Peninsula, Northwest Pacific region. In: Eichelberger J, Izbekov P, Ruppert N, Lees J, Gordeev E (eds) *Volcanism and subduction: the Kamchatka Region*. AGU Geophysical Monograph Series, vol 172, pp 165–198
- Ponomareva VV, Kyle PR, Pevzner MM, Sulerzhitsky LD, Hartman M (2007b) Holocene eruptive history of Shiveluch volcano. Kamchatka Peninsula. In: Eichelberger J, Izbekov P, Ruppert N, Lees J, Gordeev E (Eds) *Volcanism and subduction: the Kamchatka Region*. AGU Geophysical Monograph Series, vol 172, pp 263–282
- Portnyagin M, Ponomareva V (2012) Kliuchevskoi volcano diary. *Int J Earth Sci (Geol Rundsch)* 101:195
CrossRef
- Portnyagin M, Bindeman I, Hoernle K, Hauff F (2007) Geochemistry of primitive lavas of the Central Kamchathan Depression: Magma generation at the edge of the Pacific Plate. In: Eichelberger J, Gordeev E, Kasahara M, Izbekov P, Lees J (Eds) *Volcanism and subduction: the Kamchatka Region*. AGU Geophysical Monograph Series, vol 172, pp 199–239
- Portnyagin M, Ponomareva V, Bindeman I, Hauff F, Krasheninnikov S, Kuvikas O, Mironov N, Pletchova A, van den Bogaard C, Hoernle K (2009) Millennial variations of major and trace element and isotope compositions of Klyuchevskoy magmas, Kamchatka. *Terra Nostra* 1:64–65
- Pyle DM (1995) Mass and energy budgets of explosive volcanic eruptions. *Geophys Res Lett* 5:563–566
CrossRef

Pyle DM (2000) Sizes of volcanic eruptions. In: Sigurdsson H et al (eds) Encyclopedia of volcanoes. Academic Press, London, pp 263–269

Reimer PJ, Baillie MGL, Bard E, Bayliss A, Beck JW, Blackwell PG, Bronk Ramsey C, Buck CE, Burr GS, Edwards RL, Friedrich M, Grootes PM, Guilderson TP, Hajdas I, Heaton TJ, Hogg AG, Hughen KA, Kaiser KF, Kromer B, McCormac FG, Manning SW, Reimer RW, Richards DA, Southon JR, Talamo S, Turney CSM, van der Plicht J, Weyhenmeyer CE (2009) IntCal09 and Marine09 radiocarbon age calibration curves, 0–50,000 years cal BP. Radiocarbon 51:1111–1150

Rose WI, Durant AJ (2009) Fine ash content of explosive eruptions. J Volcanol Geotherm Res 186:32–39

CrossRef

Selyangin OB, Ponomareva VV (1999) Gorelovsky volcanic center, South Kamchatka: structure and evolution. Volcanol Seismol 21(2):163–194

Shane Ph, Nairn IA, Smith VC (2005) Magma mingling in the ~50 ka Rotoiti eruption from Okataina Volcanic Centre: implications for geochemical diversity and chronology of large volume rhyolites. J Volcanol Geotherm Res 139:295–313

CrossRef

Shiraiwa T, Muraviev YaD, Kameda T, Nishio F, Toyama Y, Takahashi A, Ovsyannikov AA, Salamatin AN, Yamagata K (2001) Characteristics of a crater glacier at Ushkovsky volcano, Kamchatka, Russia, as revealed by the physical properties of ice cores and borehole thermometry. J Glaciol 47(158):423–432

CrossRef

Siebert L, Simkin T (2002) Volcanoes of the World: an Illustrated Catalog of Holocene Volcanoes and their Eruptions. Smithsonian Institution, Global Volcanism Program, Digital Information Series, GVP-3. <http://www.volcano.si.edu/world/>

Sikes EL, Samson CR, Guilderson TP, Howard WR (2000) Old radiocarbon ages in the southwest Pacific Ocean during the last glacial period and deglaciation. Nature 405(6786):555–559

CrossRef

Stuiver M, Braziunas TF (1993) Modelling atmospheric ^{14}C influences and ^{14}C ages of marine samples to 10,000 BC. Radiocarbon 35(1):137–189

Stuiver M, Reimer PJ (1986) Radiocarbon calibration program CALIB REV6.0.0 www.calib.org

Stuiver M, Reimer PJ (1993) Extended ^{14}C database and revised CALIB radiocarbon calibration

program. Radiocarbon 35:215–230

Thornalley DJR, McCave IN, Elderfield H (2011) Tephra in deglacial ocean sediments south of Iceland: stratigraphy, geochemistry and oceanic reservoir ages. J Quat Sci 26(2):190–198

[CrossRef](#)

Volynets ON (1994) Geochemical types, petrology and genesis of Late Cenozoic volcanic rocks from the Kurile-Kamchatka island-arc system. Int Geol Rev 36(4):373–405

[CrossRef](#)

Over 9 million scientific documents at your fingertips
© Springer International Publishing AG, Part of Springer Science+Business Media